E-ISSN: 3023-784X

Advanced Radiology and Imaging

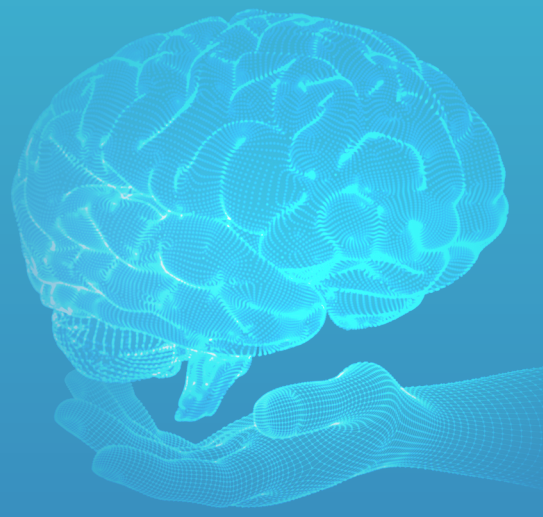

VOLUME 1 / ISSUE 2
AUGUST 2024

galenos Publishing House
ARI
advradiology.org

advradiology.org

Advanced Radiology and Imaging

VOLUME 1 / ISSUE 2
AUGUST 2024

EDITORIAL BOARD

VOLUME 1 / ISSUE 2
AUGUST
2024

Advanced Radiology and Imaging

advradiology.org

Please refer to the journal's webpage (**https://advradiology.org/**) for "**Journal Policy**" and "**Instructions to Authors**".

The editorial and publication process of the Advanced Radiology and Imaging are shaped in accordance with the guidelines of the **ICMJE, WAME, CSE, COPE, EASE,** and **NISO**. The journal is in conformity with the Principles of Transparency and Best Practice in Scholarly Publishing.

Advanced Radiology and Imaging is indexed in **Türkiye Citation Index** and **IdealOnline**.

The journal is published online.

Owner: Galenos Publishing House

Responsible Manager: Sonay Aydın

Publisher Contact
Address: Molla Gürani Mah. Kaçamak Sk. No: 21/1 34093 İstanbul, Turkey
Phone: +90 (530) 177 30 97 / +90 (539) 307 32 03
E-mail: info@galenos.com.tr/yayin@galenos.com.tr
Web: www.galenos.com.tr
Publisher Certificate Number: 14521

Publication Date: August 2024
E-ISSN: 3023-784X
International scientific journal published quarterly.

advradiology.org

Advanced Radiology and Imaging

VOLUME 1 / ISSUE 2
AUGUST 2024

CONTENTS

REVIEW

DOI: 10.4274/AdvRadiolImaging.galenos.2024.18291
Adv Radiol Imaging 2024;1(2):20-7

Idiopathic Granulomatous Mastitis: Overview and Imaging Findings

Zeycan Kübra Cevval, Baki Hekimoğlu

University of Health Sciences Turkey, Dışkapı Yıldırım Beyazıt Training and Research Hospital, Clinic of Radiology, Ankara, Turkey

Abstract

Idiopathic granulomatous mastitis (IGM) is a benign inflammatory breast disease characterized by non-caseating granulomas in the lobules of breast tissue. IGM primarily affects women of childbearing age. The actual prevalence of IGM is unknown although it is considered rare. Although the exact cause remains unclear, various triggers, such as autoimmunity, hormonal factors, and infectious agents, are believed to play a role in its pathophysiology. Imaging techniques, particularly ultrasound (US) and mammography, play vital roles in the preliminary diagnosis. The most common imaging findings are focal asymmetry on mammography and hypoechoic lesions that tend to coalesce and form tubular extensions on US. Advanced imaging techniques, including elastography and magnetic resonance imaging, can aid in diagnosis, although none of these findings are pathognomonic, necessitating histopathological evaluation for definitive diagnosis. Unlike infectious mastitis, antibiotics are not recommended for the treatment of IGM unless there is an accompanying bacterial infection. IGM should be considered in patients with mastitis that does not resolve despite prolonged antibiotic treatment. Corticosteroids are an effective first-line therapy for patients with histopathologically proven symptomatic IGM. Accurate diagnosis and treatment are crucial because of the potential for IGM findings to be mistaken for malignancy. This review discusses the general characteristics and imaging findings of IGM based on the current literature.

Keywords: Idiopathic granulomatous mastitis, ultrasound, mammography, magnetic resonance imaging, breast elastography, differential diagnosis

Introduction

Idiopathic granulomatous mastitis (IGM), also known as non-puerperal mastitis or granulomatous lobular mastitis, was first described in 1972 by Kessler and Wolloch.[1] IGM is a rare, chronic, inflammatory benign breast disease. This condition predominantly affects women of childbearing age, particularly in developing countries, and often occurs postpartum or during lactation.[2-4] Although the etiology of IGM remains unclear, it has been suggested to be associated with autoimmune processes.[2,5,6]

Clinically, IGM presents with symptoms such as pain, inflammation, erythema, and a palpable mass, with the latter being the most common. The clinical and radiological features of IGM often overlap with those of breast cancer and various benign inflammatory breast diseases, leading to frequent misdiagnosis and delayed treatment.

Ultrasound (US) and mammography play significant roles in the diagnosis of IGM. However, due to the non-specific nature of imaging findings, definitive diagnosis generally requires histopathological evaluation and exclusion of other conditions.[7]

There are various treatment options for IGM, including surgical resection, abscess drainage, steroids, methotrexate, and watchful waiting. However, no consensus has been established on the optimal treatment approach, which is often based on clinical experience and tailored to the patient and the severity of the disease.[8]

This review discusses imaging findings, pathophysiology, clinical presentation, and treatment approaches for IGM based on the current literature.

Etiology and Pathophysiology

In the pathophysiology of IGM, it is proposed that damage occurs in the ductal epithelial cells of the breast for various reasons. This damage leads to the leakage of luminal secretions into the lobular stroma of the breast, which subsequently triggers a local inflammatory response induced by the migration of macrophages and lymphocytes to the area, followed by the formation of a granulomatous reaction.[9]

Since the exact cause of IGM remains unclear, most cases are termed "idiopathic". However, it is believed that certain "environmental stimuli" can trigger an inflammatory granulomatous reaction, primarily in genetically predisposed individuals. There are three hypotheses that are thought to be responsible for the pathogenesis of IGM: autoimmunity, infection, and hormonal disorders.[10] Additionally, alpha-1 antitrypsin deficiency, oral contraceptives (OCs), smoking, breastfeeding, and pregnancy are considered potential predisposing factors. The presence

Cite this article as: Cevval ZK, Hekimoğlu B. Idiopathic Granulomatous Mastitis: Overview and Imaging Findings. Adv Radiol Imaging. 2024;1(2):20-7

Address for Correspondence: Zeycan Kübra Cevval MD, University of Health Sciences Turkey, Dışkapı Yıldırım Beyazıt Training and Research Hospital, Clinic of Radiology, Ankara, Turkey
Phone: +90 538 983 90 28 **E-mail:** zeycancevval@gmail.com **ORCID ID:** orcid.org/0000-0003-0523-057X
Received: 11.07.2024 **Accepted:** 08.08.2024

of multiple predisposing factors is believed to further exacerbate the disease.[8]

The effectiveness of immunomodulatory drugs, such as steroids and methotrexate, in treating IGM supports the autoimmune theory.[11,12] Furthermore, some studies have found positive anti-nuclear antibodies, rheumatoid factor, and elevated serum levels of interleukin (IL)-17, IL-22, and IL-23 in patients with IGM.[13,14]

Another hypothesis regarding the pathogenesis of IGM is infectious processes. Corynebacterium bacteria have been isolated from IGM cases, suggesting a possible role in the disease.[15] However, since these bacteria are also part of the normal skin flora of the breast, it remains debated whether the bacteria found in samples from IGM cases are contaminants or pathogens.[8,16]

Hormonal factors, such as hyperprolactinemia, are believed to be responsible for IGM recurrence and prolonged disease duration.[2] Pituitary adenomas and selective serotonin reuptake inhibitors that increase prolactin levels have also been implicated. Although it has been proposed that elevated prolactin levels lead to increased milk secretion and ductal damage, resulting in the leakage of milk secretions into the stroma and subsequent inflammatory reactions, this theory has not been definitively proven.[17,18]

IGM typically appears within 5 years postpartum and is associated with breastfeeding, with an average onset age of 33-38 years.[19]

Gurleyik et al.[21] reported that 15 out of 19 IGM patients had a history of breastfeeding, while Azizi et al.[20] found that 90.7% of 474 IGM patients had a history of pregnancy, and 82.7% of these patients had breastfed. Although pregnancy, childbirth, and breastfeeding are strongly associated with IGM, the disease is also observed in men and women aged >80 years, indicating that these factors are not fundamental pathogenic factors.[8]

OCs, similar to hyperprolactinemia, have been suggested as potential factors for IGM pathology because of their role in increasing breast secretion. Some studies have found varying percentages (21-42%) of OC use among IGM cases[21,22], whereas other studies have not demonstrated a significant relationship.[23]

In our opinion, since IGM is more frequently observed in developing countries, studies with large sample sizes are often conducted in such populations. However, the lower rates of smoking and OC use in these countries compared with the Western countries may lead to misleading results regarding potential factors.

Clinical Findings

IGM most commonly presents in women aged 30-45 years with a unilateral, palpable breast mass of varying sizes (1-20 cm). It can occur in any quadrant of the breast, but it is most frequently reported in the upper outer quadrants.[24] The palpable mass may be accompanied by skin manifestations such as erythema, nipple retraction, and a peau d'orange appearance. In chronic and severe cases, abscess formation, ulcerative appearance of the skin, and purulent discharge through sinus tracts extending to the skin may occur.[8] Additionally, ipsilateral axillary lymphadenopathy may be present in some cases.

Due to its presentation with a breast mass and skin changes, the differential diagnosis of IGM can be challenging, even with the use of mammography, US, magnetic resonance imaging (MRI), and other imaging modalities, to distinguish it from inflammatory breast cancer (IBC). Furthermore, although rare, breast tuberculosis should be considered in the differential diagnosis. However, the presence of concomitant pulmonary findings in tuberculosis, the demonstration of caseous necrosis on histopathological examination, and the involvement of breast ducts can help rule out IGM.[25] Ultimately, because IGM is rare and its clinical findings are not specific, imaging findings and histopathological examination are required for diagnosis.

Imaging Findings

In the presence of a palpable breast mass, as observed in IGM, the accepted approach is to perform US for patients under 40 years of age and mammography for patients over 40 years of age.[19] Additionally, advanced imaging techniques, such as elastography and tomosynthesis, are used in clinical practice. When US and mammography are insufficient, MRI plays a significant role in demonstrating disease extent and detecting active inflamed tissue remnants that may be obscured by edematous tissue.

Mammography

Various mammographic findings of IGM have been described, but none are pathognomonic. A review of the literature revealed that the most commonly encountered mammographic findings are irregular and poorly defined masses with focal asymmetry (Figure 1). However, it should be noted that no pathology may be detected on mammography in patients with dense breast tissue or mild symptoms in the initial stage.[19,26,27]

Additional mammographic findings included axillary lymphadenopathy, focal skin thickening or edema, and nipple retraction (Figure 2). Similar findings were observed in IBC; however, in cancer, edema involves a larger portion of the skin, whereas in IGM, focal edema affects a smaller area of the skin.[28]

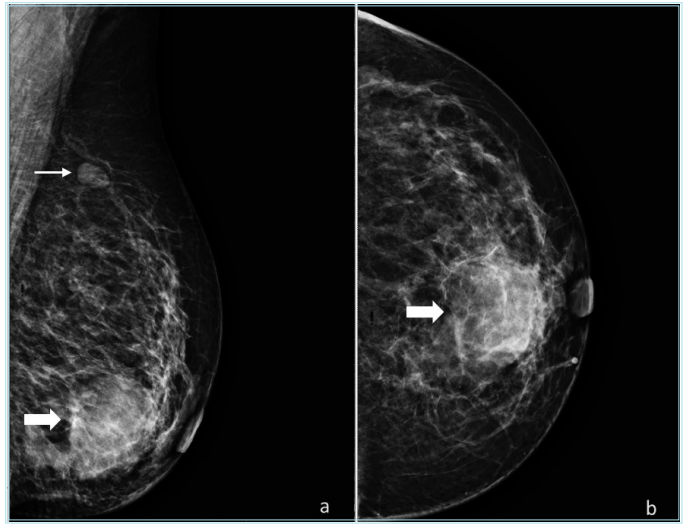

Figure 1. In the mediolateraloblique (MLO) (a) and craniocaudal (b) mammographic images of a 45-year-old female patient presenting with palpable mass and breast tenderness, an irregularly and poorly defined nodular opacity (arrows) is observed in the lower central quadrant. Additionally, the MLO view reveals a nodular appearance of a reactive intramammary lymph node (thin arrow) in the upper half (correlated with ultrasound). Pathology results reported "granulomatous mastitis"

(From the archives of Prof. Dr. Irmak Durur Subasi)

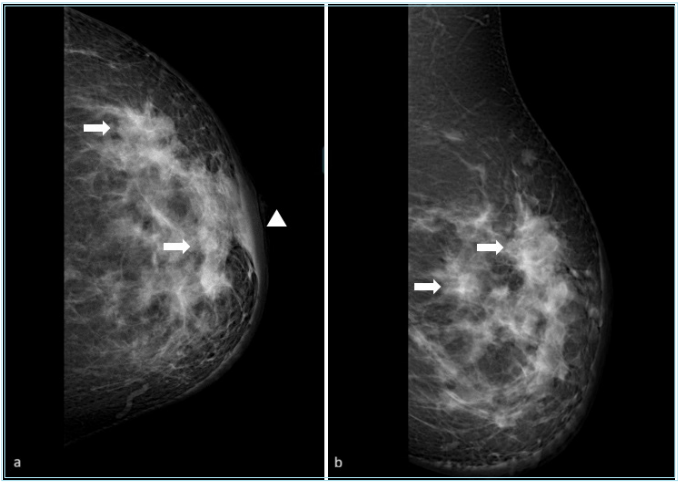

Figure 2. In the left breast craniocaudal (a) and mediolateraloblique (b) mammograms of a 39-year-old female patient, focal asymmetries are observed, with several irregularly defined nodular densities tending to coalesce, the largest in the upper outer quadrant (arrows). Associated skin thickening/edema around the areola is also present (arrowhead). Core needle biopsy pathology results indicated "granulomatous lobular mastitis"

Calcifications are not typical mammographic findings in IGM. Fazzio et al.[29] proposed that calcifications might be a rare finding in granulomatous mastitis, based on a case with segmental coarse heterogeneous calcifications. Additionally, there have been reports in the literature in which microcalcifications associated with synchronous breast cancer were masked during the active phase of IGM but were detected in follow-up mammograms after treatment. These findings suggest that post-treatment mammography is beneficial in avoiding missing synchronous cancer lesions once breast pain or tenderness subsides.[30,31]

In conclusion, although mammographic findings may raise suspicion of IGM, no pathognomonic features allow for a definitive diagnosis. Correlations with other radiologic modalities and histopathologic sampling are necessary for a definitive diagnosis.

Ultrasound

Regardless of age, US is the primary imaging modality for patients with symptoms of mastitis. US is also frequently used in IGM for image-guided biopsies and intralesional steroid treatment because of its nonradiative nature.

Although the sonographic appearance of IGM varies greatly, the most frequently reported finding is irregularly shaped hypoechoic lesions or masses with or without tubular extensions. The tubular extension and coalescing tendency of the lesions describe the reticular appearance of the disease spreading around the lobules.[7,27,32,33] The orientation of lesions is almost always parallel to the skin.[33] On Doppler US, the lesions and surrounding tissues exhibited hypervascular characteristics (Figure 3).[29,34] In the advanced stages of the disease, breast abscesses can develop, with reported prevalence in the literature ranging from 6.6% to 54.0%.[29,32,35]

Auxiliary US findings for the diagnosis of IGM include skin thickening and subcutaneous fat tissue edema, increased echogenicity of subcutaneous fat tissue secondary to inflammation, and reactive axillary lymphadenopathy with preserved fatty hilum and thick cortex. The frequency of these findings varies across studies.[12,19,33,35,36]

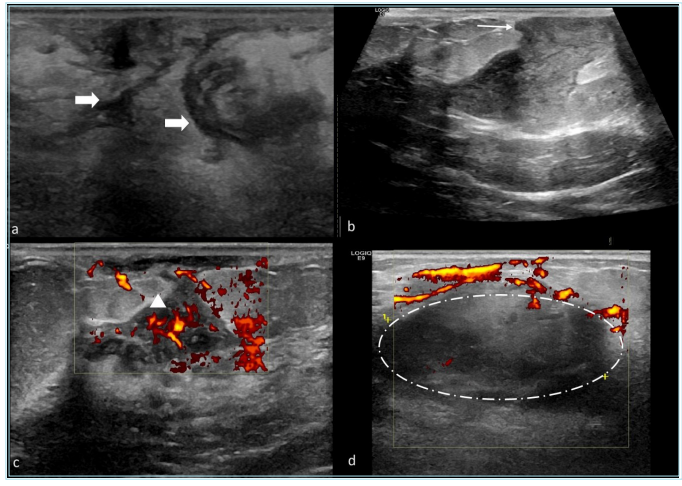

Figure 3. Ultrasonographic images from three different patients diagnosed with idiopathic granulamatous mastitis. The first image (a) shows irregular hypoechoic lesions interconnected by tubular extensions (arrows) and increased echogenicity of fat tissue due to inflammation. The images (b) and (c) display polygonal-shaped irregular hypoechoic lesions with vascularization on doppler imaging (arrowhead), extending towards the skin (thin arrow). The image (d) shows a hypoechoic round abscess focus (circled) with peripheral vascularization in the advanced stages of the disease

(From the archives of Prof. Dr. Irmak Durur Subasi)

Elastography

Elastography is an innovative complementary imaging technology that enhances the diagnostic capabilities of B-mode US by evaluating tissue stiffness. There are two primary types of elastography used to assess breast lesions: shear wave elastography (SWE) and strain elastography. Strain elastography is operator-dependent, whereas SWE, which uses focused radiation forces without manual compression, is independent of the operator. Using SWE, color-coded maps (elastograms) based on tissue stiffness are created, allowing for semi-quantitative measurements.

Studies have shown that SWE is effective in distinguishing benign from malignant breast lesions and can improve the specificity of traditional US when using the Breast Imaging Reporting and Data System (BIRADS) criteria. Elastography plays a crucial role in distinguishing BIRADS 3 from BIRADS 4A lesions in diagnosis.[37] While clinicians often use palpation to understand the elasticity of pathological tissues or masses, sonoelastography provides a more objective method, enabling more sensitive and specific differentiation between benign and malignant breast lesions based on stiffness.[38]

Various studies have investigated its efficacy in differentiating IGM from breast malignancies.[39,40] A recent study by Toprak et al.[41] explored the qualitative and quantitative roles of SWE in distinguishing IGM from invasive ductal carcinoma, obtaining 89% sensitivity and 84% specificity. Another study by Durur-Karakaya et al.[40] found that qualitative and semiquantitative elastography parameters evaluated in all IGM cases were consistent with the benign criteria. They found that sonoelastography revealed low ES and SR values and equal ED for IGM. Because these are all features of benign breast lesions, sonoelastography may be a valuable technique for the diagnosis of IGM (Figure 4).

However, Aslan et al.[42] measured the stiffness of lesions in IGM cases before and after treatment and found no significant difference. Additionally, Ece et al.[43] evaluated the feasibility of using elastography

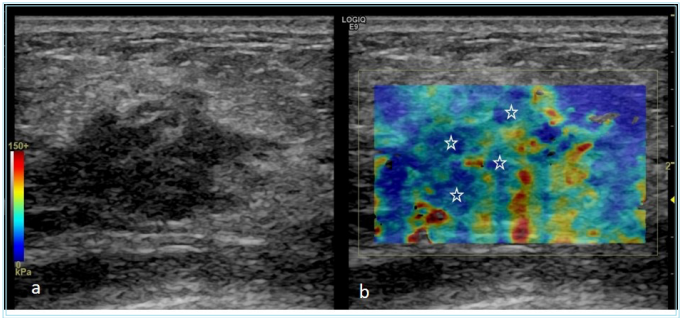

Figure 4. In a patient diagnosed with idiopathic granulamatous mastitis, a hypoechoic patchy area is observed on gray-scale ultrasound (a), and free-hand elastography reveals that the lesion predominantly consists of soft areas coded in blue (stars). In contrast, malignant masses typically appear as stiffer structures on elastography

(From the archive of Prof. Dr. Irmak Durur Subasi)

to adjust corticosteroid doses in the treatment of IGM, noting that the use of SWE may allow for lower corticosteroid dosages. More studies are needed to demonstrate the value of SWE in predicting clinical response to IGM.

Magnetic Resonance Imaging

MRI is typically used in specific scenarios where US and mammography are insufficient for decision-making, to determine lesion extent, assist with biopsy, and to evaluate auxiliary extramammary findings. Additionally, MRI is useful for assessing suspicious residual inflammatory areas. Although MRI is less frequently used compared with US and mammography, its sensitivity and high positive predictive value make it a valuable tool.[12,27,29,30,44,45]

IGM MRI findings, like those on US and mammography findings, vary significantly. When evaluating the MRI characteristics of breast lesions, the edge features of the lesions are of primary importance. Although malignant breast lesions typically have spiculated and irregular edges, benign breast lesions usually have smooth or lobulated edges. IGM is an exception, as its lesion contours can be smooth, lobulated, or spiculated despite being benign, necessitating advanced imaging with contrast-enhanced MRI.[46-48]

In MRI, IGM shows focal or diffuse asymmetric signal enhancement and contrast uptake. The most common pattern observed is hyperintense signal on T2-weighted images (WI), hypointense signal on T1WI, with segmental heterogeneity and irregular contrast-enhancing lesions (Figure 5). Nodular lesions and abscesses can also be observed. The severity of the inflammatory reaction and the amount of fibrotic content in IGM vary over time, leading to different MRI findings depending on the phase. For example, aseptic abscess formation, thought to develop via an autoimmune mechanism, can be observed in a certain phase of IGM. IGM lesions show heterogeneous, diffuse, or nodular contrast enhancement patterns, and peripheral contrast enhancement is observed in abscesses (Figure 6). Although IGM lesions typically exhibit a type 1 benign contrast-enhancement pattern in post-contrast dynamic series, they have occasionally been reported to show a type 3 malignant contrast-enhancement pattern.[7,26,46,49]

In diffusion MRI, abscess foci in IGM can show diffusion restriction with low ADC values, necessitating differentiation from malignancy. In MRI spectroscopy, a choline peak is observed in malignant lesions, whereas this peak is not seen in IGM abscesses.[50] Additionally, the peripheral contrast enhancement pattern of abscesses aids in distinguishing them from malignancies.

IGM and Differential Diagnosis

IGM is challenging to diagnose due to similarities to malignancies and other inflammatory breast diseases. Definitive diagnosis is achieved through clinical history, examination findings, imaging results, and histopathological examination, making IGM a diagnosis of exclusion.

The primary diseases to consider in the differential diagnosis of IGM are IBC, infective mastitis, breast tuberculosis, diabetic fibrous mastopathy, foreign body granulomas, and sarcoidosis (Table 1).[7]

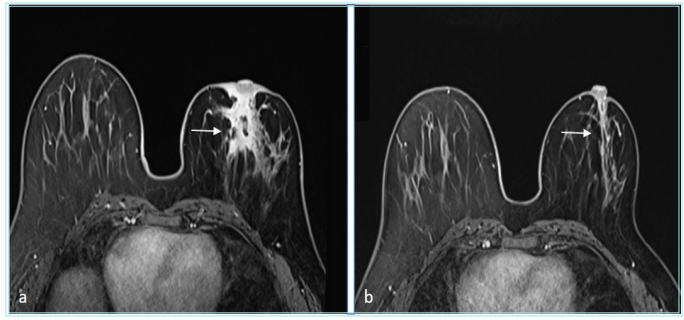

Figure 5. Post-contrast T1-weighted (T1W) breast magnetic resonance images of a 38-year-old female patient show a heterogeneous irregularly shaped area of enhancement in the right retroareolar region (a), one year after treatment follow-up images of the same patient (b), show near-complete regression of the findings (thin arrows). The pathology result confirmed "granulamatous mastitis"

(From the archive of Prof. Dr. Irmak Durur Subasi)

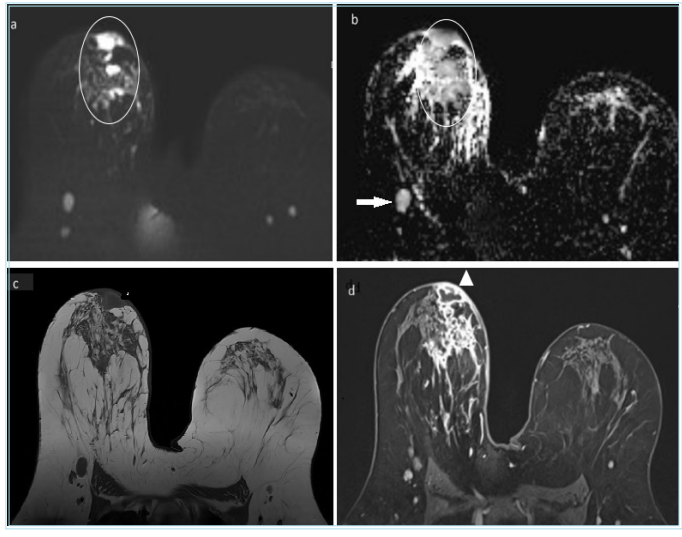

Figure 6. In the dynamic contrast-enhanced magnetic resonance images of a 30-year-old female patient, diffusion-weighted images (a) and ADC images (b) show diffusion restrictions in the abscess foci in the left breast (circled), which appear to be coalescing. In the T1W pre-contrast (c) and post-contrast series (d), peripheral enhancement is observed in the abscess foci (arrowhead), along with heterogeneously irregularly shaped enhancing lesions in other sections. Additionally, a few reactive lymph nodes are observed in the left axillary tail (arrow)

Table 1. Typical clinical and imaging-based differential diagnoses for IGM

Diagnosis	Demographics and clinical manifestations	Imaging findings	Histopathologic features
IGM	- Mainly affects premenopausal and parous women - Palpable mass, mastalgia with or without mild focal skin erythema or draining sinus, history of failed antibiotic treatments	**MG:** focal asymmetric density or irregular mass, trabecular and skin thickening. **US:** irregular hypoechoic mass with hypoechoic tubular extensions. **MRI:** heterogeneous enhancing T2-hyperintense mass and/or rim-enhancing lesions with non-mass enhancement.	- Lobulocentric non-caseating granulomas - Negative microbial staining and culture results.
IBC	- Mainly affects older women (average age, 58 years, as compared with 33 years for IGM group) - Skin erythema in at least one-third of the breast, peau d'orange, asymmetric breast engorgement, onset to manifestation of symptoms less than 3 months, axillary adenopathy in approximately 50-85% of cases.	**MG:** skin and trabecular thickening, asymmetric increased breast density with or without focal asymmetry, irregularly shaped mass, axillary adenopathy. **US:** extensive skin thickening and breast edema, dilated lymphatics, axillary adenopathy, heterogeneous parenchyma with or without suspicious or conglomerate masses. **MRI:** breast and chest wall edema, streaky T2 hyperintensity, dilated lymphatics, skin enhancement, contiguous or coalescent irregular breast masses with rapid enhancement and washout kinetics (type 3).	-Most often invasive ductal carcinoma that is poorly differentiated, with dermal lymphovascular invasion - No inflammation
Infective mastitis	- Common in females of reproductive age, but seen in persons of all ages - Non-cyclical breast pain and/or tenderness, erythema, fever with or without abscess - Clinical unresponsiveness to empiric antibiotics in the presence of positive microbial stains and/or cultures suggests an atypical or resistant organism.	**MG:** (often not performed): trabecular and skin thickening, asymmetric increasedbreast density. **US:** diffuse or focal skin thickening, inhomogeneous breast tissue with or without irregular hypoechoic mass (with or without fluid collection) (particularly lactation mastitis).	- Abundant leukocytes - Positive microbial staining and culture results, with *Staphylococcus* and *Streptococcus bacteria* often seen inspissated secretions - Atypical organisms for which additional staining is required for identification may be seen
Tuberculous mastitis	- Seen in endemic areas, high-risk populations, and persons with a history of pulmonary tuberculosis (50% of cases) - Palpable breast mass, axillary lymphadenopathy, unilateral involvement, less mastalgia compared with IGM	**MG:** findings similar to those of infectious mastitis. **US:** heterogeneous hypoechoic irregularmass, axillary lymphadenopathy with or without fluid collections.	- Caseating granulomas - Positive acid-fast or fite staining results

MG: Mamography, US: Ultrasound, MRI: Magnetic resonance imaging, IGM: Idiopatic granulamatous mastitis, IBC: Inflammatory breast cancer

IGM and Artificial Intelligence

Artificial intelligence (AI) is a modern technical discipline rooted in mathematics and computer science. It focuses on developing theories, methods, and application systems to simulate and enhance human intelligence.

Breast imaging offers distinctive features that present valuable opportunities for AI applications. The BIRADS from the American College of Radiology, with its well-established and structured lexicon, is particularly instrumental in advancing AI development and implementation. BI-RADS provides a standardized system for terminology, reporting, classification, communication, and medical auditing across mammography, breast US, and breast MRI.[51] This standardized framework is crucial for the growth and assessment of AI in breast imaging, especially by offering a predefined methodology for radiologists to interpret imaging studies and map results.[52]

There are studies in the literature that use AI to distinguish IGM from breast cancer. In a recent study, deep learning-based automatic classification systems were found to be reliable auxiliary methods for distinguishing between non-lactating mastitis and malignant breast tumors, with high sensitivity, accuracy, and specificity.[53]

Another publication demonstrated that a nomogram combining radionic and US features exhibited good diagnostic performance in distinguishing between IGM and IBC, suggesting that it could be used as a non-invasive diagnostic method.[54]

Deep Learning Radiomic Nomogram, developed based on radionic and deep learning features of US images, has been noted to have potential clinical value in effectively differentiating between mass mastitis (MM) and IBC. As the system evolves into an autonomous screening system, it is expected to improve MM diagnosis rates in rural hospitals and reduce the likelihood of incorrect treatment and overtreatment.[55]

In another publication, investigating the role of AI in distinguishing benign inflammatory breast lesions from malignant processes indicated that AI produced results comparable to radiologists' US reports for benign inflammatory diseases and demonstrated high reliability within itself. These findings suggest that AI could be considered for use in the diagnosis of granulomatous mastitis and similar inflammatory breast diseases.[56]

Treatment

There is no consensus in the literature regarding the treatment of IGM. Various treatment options are discussed, including surgical resection, steroids, methotrexate, bromocriptine, colchicine, immunosuppressive agents, antibiotics, and even conservative follow-up. Currently, treatment largely depends on the clinician's or surgeon's experience and the severity of the patient's disease.[8,57]

Although surgical excision has been widely accepted as the most common treatment for IGM, it is now considered a last resort due to the potential for recurrence, cosmetic issues, and the development of fistulas in the postoperative period.[33]

In recent years, medical treatment, particularly steroid therapy, has been recommended as first-line treatment.[58] Numerous studies in the literature have shown that oral or local (or combined) steroid therapy can alleviate preoperative symptoms and can be used as a definitive treatment option with low recurrence rates. In particular, intralesional steroid therapy has been compared with other treatment methods because it reduces the side effects associated with systemic use and provides targeted bolus therapy. It has been suggested that a quicker treatment response can be achieved, and even severe cases can be managed with monotherapy.[36,58-62] The primary adverse effect of intralesional steroid therapy is skin atrophy.

Studies by Bouton et al.[63] and Davis et al.[64] have suggested that a conservative follow-up approach should be considered, especially in mild cases. However, some studies reported frequent recurrence in these cases.[65]

Additionally, a recent study by Sarkar et al.[66] found that wide local excision with ductal excision is the best curative treatment for patients with recurrent disease who do not respond to conservative therapy.

Conclusion

IGM is a benign inflammatory breast disease characterized by non-caseating granulomas in the lobules of breast tissue. IGM most commonly affects women of childbearing age. Imaging techniques, particularly US and mammography, play crucial roles in the preliminary diagnosis. Advanced imaging techniques, including elastography and MRI, can assist in diagnosis, although none of these findings are pathognomonic, necessitating histopathological evaluation for definitive diagnosis. IGM is a rare but chronic disease that is difficult to treat and must be definitively diagnosed because of its potential to be mistaken for malignancies. Therefore, standardized diagnosis and treatment protocols based on new studies are needed.

Acknowledgment

I would like to express my deep gratitude to Prof. Dr. Irmak Subaşı for her help and support.

Note: All figures used are original, and written consent has been obtained from the relevant patients for the use of these figures.

Ethics

Authorship Contributions

Concept: Z.K.C., B.H., Design: Z.K.C., B.H., Data Collection or Processing: Z.K.C., Analysis or Interpretation: Z.K.C., B.H., Literature Search: Z.K.C., Writing: Z.K.C.

Conflict of Interest: No conflict of interest was declared by the authors.

Financial Disclosure: The authors declared that this study received no financial support.

References

1. Kessler E, Wolloch Y. Granulomatous mastitis: a lesion clinically simulating carcinoma. Am J Clin Pathol. 1972;58:642-6.
2. Erhan Y, Veral A, Kara E, et al. A clinicopthologic study of a rare clinical entity mimicking breast carcinoma: idiopathic granulomatous mastitis. Breast. 2000;9:52-6.
3. Bani-Hani KE, Yaghan RJ, Matalka II, Shatnawi NJ. Idiopathic granulomatous mastitis: time to avoid unnecessary mastectomies. Breast J. 2004;10:318-22.
4. Nikolaev A, Blake CN, Carlson DL. Association between Hyperprolactinemia and Granulomatous Mastitis. Breast J. 2016;22:224-31.
5. Akbulut S, Yilmaz D, Bakir S. Methotrexate in the management of idiopathic granulomatous mastitis: review of 108 published cases and report of four cases. Breast J. 2011;17:661-8.
6. Boufettal H, Essodegui F, Noun M, Hermas S, Samouh N. Idiopathic granulomatous mastitis: a report of twenty cases. Diagn Interv Imaging. 2012;93:586-96.
7. Pluguez-Turull CW, Nanyes JE, Quintero CJ, et al. Idiopathic Granulomatous Mastitis: Manifestations at Multimodality Imaging and Pitfalls. Radiographics. 2018;38:330-56.
8. Yin Y, Liu X, Meng Q, Han X, Zhang H, Lv Y. Idiopathic Granulomatous Mastitis: Etiology, Clinical Manifestation, Diagnosis and Treatment. J Invest Surg. 2022;35:709-20.
9. Altintoprak F, Karakece E, Kivilcim T, et al. Idiopathic granulomatous mastitis: an autoimmune disease? ScientificWorldJournal. 2013;2013:148727.
10. Sheybani F, Naderi HR, Gharib M, Sarvghad M, Mirfeizi Z. Idiopathic granulomatous mastitis: Long-discussed but yet-to-be-known. Autoimmunity. 2016;49:236-9.
11. Sheybani F, Sarvghad M, Naderi H, Gharib M. Treatment for and clinical characteristics of granulomatous mastitis. Obstet Gynecol. 2015;125:801-7.
12. Gautier N, Lalonde L, Tran-Thanh D, et al. Chronic granulomatous mastitis: Imaging, pathology and management. Eur J Radiol. 2013;82:e165-75.
13. Saydam M, Yilmaz KB, Sahin M, et al. New Findings on Autoimmune Etiology of Idiopathic Granulomatous Mastitis: Serum IL-17, IL-22 and IL-23 Levels of Patients. J Invest Surg. 2021;34:993-7.
14. Ozel L, Unal A, Unal E, et al. Granulomatous mastitis: is it an autoimmune disease? Diagnostic and therapeutic dilemmas. Surg Today. 2012;42:729-33.
15. Mathelin C, Riegel P, Chenard MP, Tomasetto C, Brettes JP. Granulomatous mastitis and corynebacteria: clinical and pathologic correlations. Breast J. 2005;11:357.
16. Paviour S, Musaad S, Roberts S, et al. Corynebacterium species isolated from patients with mastitis. Clin Infect Dis. 2002;35:1434-40.
17. Cserni G, Szajki K. Granulomatous Lobular Mastitis Following Drug-Induced Galactorrhea and Blunt Trauma. Breast J. 1999;5:398-403.
18. Bellavia M, Damiano G, Palumbo VD, et al. Granulomatous Mastitis during Chronic Antidepressant Therapy: Is It Possible a Conservative Therapeutic Approach? J Breast Cancer. 2012;15:371-2.
19. Hovanessian Larsen LJ, Peyvandi B, Klipfel N, Grant E, Iyengar G. Granulomatous lobular mastitis: imaging, diagnosis, and treatment. AJR Am J Roentgenol. 2009;193:574-81.
20. Azizi A, Prasath V, Canner J, et al. Idiopathic granulomatous mastitis: Management and predictors of recurrence in 474 patients. Breast J. 2020;26:1358-62.
21. Gurleyik G, Aktekin A, Aker F, Karagulle H, Saglamc A. Medical and surgical treatment of idiopathic granulomatous lobular mastitis: a benign

inflammatory disease mimicking invasive carcinoma. J Breast Cancer. 2012;15:119-23.

22. Oran EŞ, Gürdal SÖ, Yankol Y, et al. Management of idiopathic granulomatous mastitis diagnosed by core biopsy: a retrospective multicenter study. Breast J. 2013;19:411-8.
23. Baslaim MM, Khayat HA, Al-Amoudi SA. Idiopathic granulomatous mastitis: a heterogeneous disease with variable clinical presentation. World J Surg. 2007;31:1677-81.
24. Naraynsingh V, Hariharan S, Dan D, Harnarayan P, Teelucksingh S. Conservative management for idiopathic granulomatous mastitis mimicking carcinoma: case reports and literature review. Breast Dis. 2010;31:57-60.
25. Seo HR, Na KY, Yim HE, et al. Differential diagnosis in idiopathic granulomatous mastitis and tuberculous mastitis. J Breast Cancer. 2012;15:111-8.
26. Dursun M, Yilmaz S, Yahyayev A, et al. Multimodality imaging features of idiopathic granulomatous mastitis: outcome of 12 years of experience. Radiol Med. 2012;117:529-38.
27. Oztekin PS, Durhan G, Nercis Kosar P, Erel S, Hucumenoglu S. Imaging Findings in Patients with Granulomatous Mastitis. Iran J Radiol. 2016;13:e33900.
28. Tardivon AA, Viala J, Corvellec Rudelli A, Guinebretiere JM, Vanel D. Mammographic patterns of inflammatory breast carcinoma: a retrospective study of 92 cases. Eur J Radiol. 1997;24:124-30.
29. Fazzio RT, Shah SS, Sandhu NP, Glazebrook KN. Idiopathic granulomatous mastitis: imaging update and review. Insights Imaging. 2016;7:531-9.
30. Alper F, Abbasguliyev H, Özmen S, Yalçin A, Yılmaz Çankaya B, Akçay MN. Clinical, Histopathological, Imaging, and Treatment Perspectives of Inflammatory Granulomatous Mastitis: Review of the Literature. Eurasian J Med. 2022;54(Suppl 1):172-8.
31. An JK, Woo JJ, Lee SA. Non-puerperal mastitis masking pre-existing breast malignancy: importance of follow-up imaging. Ultrasonography. 2016;35:159-63.
32. Yildiz S, Aralasmak A, Kadioglu H, et al. Radiologic findings of idiopathic granulomatous mastitis. Med Ultrason. 2015;17:39-44.
33. Lee JH, Oh KK, Kim EK, Kwack KS, Jung WH, Lee HK. Radiologic and clinical features of idiopathic granulomatous lobular mastitis mimicking advanced breast cancer. Yonsei Med J. 2006;47:78-84.
34. Handa P, Leibman AJ, Sun D, Abadi M, Goldberg A. Granulomatous mastitis: changing clinical and imaging features with image-guided biopsy correlation. Eur Radiol. 2014;24:2404-11.
35. Al-Khawari HA, Al-Manfouhi HA, Madda JP, Kovacs A, Sheikh M, Roberts O. Radiologic features of granulomatous mastitis. Breast J. 2011;17:645-50.
36. Aghajanzadeh M, Hassanzadeh R, Alizadeh Sefat S, et al. Granulomatous mastitis: Presentations, diagnosis, treatment and outcome in 206 patients from the north of Iran. Breast. 2015;24:456-60.
37. Balleyguier C, Ciolovan L, Ammari S, et al. Breast elastography: the technical process and its applications. Diagn Interv Imaging. 2013;94:503-13.
38. Barr RG, Destounis S, Lackey LB, Svensson WE, Balleyguier C, Smith C. Evaluation of breast lesions using sonographic elasticity imaging: a multicenter trial. J Ultrasound Med. 2012;31:281-7.
39. Pu H, Zhang XL, Xiang LH, et al. The efficacy of added shear wave elastography (SWE) in breast screening for women with inconsistent mammography and conventional ultrasounds (US). Clin Hemorheol Microcirc. 2019;71:83-94.
40. Durur-Karakaya A, Durur-Subasi I, Akcay MN, Sipal S, Guvendi B. Sonoelastography findings of idiopathic granulomatous mastitis. Jpn J Radiol. 2015;33:33-8.
41. Toprak N, Toktas O, Ince S, et al. Does ARFI elastography complement B-mode ultrasonography in the radiological diagnosis of idiopathic granulomatous mastitis and invasive ductal carcinoma? Acta Radiol. 2022;63:28-34.
42. Aslan H, Arer IM, Pourbagher A, Ozen M. Is there a correlation between the severity of Idiopathic Granulomatous Mastitis and pre-treatment Shear-Wave Elastography Findings? Original research. Ann Ital Chir. 2018;89:489-94.
43. Ece B, Aydin S, Kantarci M. Shear Wave Elastography-Correlated Dose Modifying: Can We Reduce Corticosteroid Doses in Idiopathic Granulomatous Mastitis Treatment? Preliminary Results. J Clin Med. 2023;12:2265.
44. Poyraz N, Emlik GD, Batur A, Gundes E, Keskin S. Magnetic Resonance Imaging Features of Idiopathic Granulomatous Mastitis: A Retrospective Analysis. Iran J Radiol. 2016;13:e20873.
45. Durur-Subasi I, Durur-Karakaya A, Alper F, et al. Breast lesions with high signal intensity on T1-weighted MR images. Jpn J Radiol. 2013;31:653-61.
46. Anik Y. Radiological Findings of Idiopathic Granulomatous Mastitis: Review. TURKIYE KLINIKLERI TIP BILIMLERI DERGISI. 2010;30:286-92.
47. Lo GG, Ai V, Chan JK, et al. Diffusion-weighted magnetic resonance imaging of breast lesions: first experiences at 3 T. J Comput Assist Tomogr. 2009;33:63-9.
48. Yanık B, Gümüş M, Sak SD, Hekimoğlu B. İdiyopatik granülomatöz mastit: görüntüleme bulguları. Tanısal ve Girişimsel Radyoloji. 2002;8:372-6.
49. Cakir B, Tuncbilek N, Karakas HM, Unlu E, Ozyilmaz F. Granulomatous mastitis mimicking breast carcinoma. Breast J. 2002;8:251-2.
50. Anik Y, Inan N, Sarisoy HT, Arslan AS, Demirci A. MR imaging and MR spectroscopy findings of multiple breast abscess in the nonlactating case. Breast J. 2007;13:527-8.
51. Sickles EA. ACR BI-RADS® Atlas, Breast imaging reporting and data system. American College of Radiology. 2013:39.
52. Taylor CR, Monga N, Johnson C, Hawley JR, Patel M. Artificial Intelligence Applications in Breast Imaging: Current Status and Future Directions. Diagnostics (Basel). 2023;13:2041.
53. Zhou Y, Feng BJ, Yue WW, et al. Differentiating non-lactating mastitis and malignant breast tumors by deep-learning based AI automatic classification system: A preliminary study. Front Oncol. 2022;12:997306.
54. Ma Q, Lu X, Qin X, et al. A sonogram radiomics model for differentiating granulomatous lobular mastitis from invasive breast cancer: a multicenter study. Radiol Med. 2023;128:1206-16.
55. Wu L, Li S, Wu C, Wu S, Lin Y, Wei D. Ultrasound-based deep learning radiomics nomogram for differentiating mass mastitis from invasive breast cancer. BMC Med Imaging. 2024;24:189.
56. Durur-Subasi I, Eren A, Gungoren FZ, et al. Evaluation of pathologically confirmed benign inflammatory breast diseases using artificial intelligence on ultrasound images. Revista de Senología y Patología Mamaria. 2024;37:100558.
57. Ma X, Min X, Yao C. Different Treatments for Granulomatous Lobular Mastitis: A Systematic Review and Meta-Analysis. Breast Care (Basel). 2020;15:60-6.
58. Toktas O, Toprak N, Elasan S, Calli I, Binici S. Treatment of Idiopathic Granulomatous Mastitis: Local Steroid Administration vs. Systemic (Oral) Steroid. Indian J Surg. 2023;85:350-6.
59. Yuan QQ, Xiao SY, Farouk O, et al. Management of granulomatous lobular mastitis: an international multidisciplinary consensus (2021 edition). Mil Med Res. 2022;9:20.
60. Alper F, Karadeniz E, Güven F, et al. Comparison of the Efficacy of Systemic Versus Local Steroid Treatment in Idiopathic Granulomatous Mastitis: A Cohort Study. J Surg Res. 2022;278:86-92.
61. Gunduz Y, Altintoprak F, Tatli Ayhan L, Kivilcim T, Celebi F. Effect of topical steroid treatment on idiopathic granulomatous mastitis: clinical and radiologic evaluation. Breast J. 2014;20:586-91.
62. Munot K, Nicholson S, Birkett V. Granulomatous mastitis: A novel method of treatment. EJSO. 2012;38:461-62.
63. Bouton ME, Jayaram L, O'Neill PJ, Hsu CH, Komenaka IK. Management of idiopathic granulomatous mastitis with observation. Am J Surg. 2015;210:258-62.

64. Davis J, Cocco D, Matz S, et al. Re-evaluating if observation continues to be the best management of idiopathic granulomatous mastitis. Surgery. 2019;166:1176-80.

65. Yabanoğlu H, Çolakoğlu T, Belli S, et al. A Comparative Study of Conservative versus Surgical Treatment Protocols for 77 Patients with Idiopathic Granulomatous Mastitis. Breast J. 2015;21:363-9.

66. Sarkar DK, Banerjee R, Gupta S, Singhal AK, Halder A. Management of idiopathic granulomatous mastitis: a prospective study. Ann R Coll Surg Engl. 2023;105:218-24.

RESEARCH ARTICLE

DOI: 10.4274/AdvRadiolImaging.galenos.2024.25733
Adv Radiol Imaging 2024;1(2):28-32

Retrospective Evaluation of Magnetic Resonance Imaging Findings for BI-RADS 5 Lesions: A 5-year Clinical Experience

Zeliha Coşgun, Emine Dağıstan

Bolu Abant İzzet Baysal University Faculty of Medicine, Department of Radiology, Bolu, Turkey

Abstract

Objectives: This study aimed to evaluate the diagnostic utility of magnetic resonance imaging (MRI) for breast cancer detection, focusing specifically on Breast Imaging-Reporting and Data System (BI-RADS) 5 lesions. The study investigated the morphological and dynamic characteristics of these lesions using MRI to identify features associated with malignancy.

Methods: A retrospective analysis was conducted on breast MRI scans performed between January 2019 and December 2023. The study included 120 patients with BI-RADS 5 lesions who underwent biopsy or surgical excision. MRI images were evaluated for breast parenchymal patterns, T2-weighted signal characteristics, lesion size, location, enhancement kinetics, and morphological features using a standardized protocol. Histopathological results were correlated with MRI findings.

Results: Among the 120 BI-RADS 5 lesions, 109 were malignant and 11 benign. Malignant lesions predominantly exhibited heterogeneous enhancement patterns (69.7%) and hypointense T2-weighted signals (56%). Most malignant lesions (82.3%) showed washout enhancement kinetics. Benign lesions, on the other hand, exhibited predominantly hyperintense T2-weighted signals (63.6%) and heterogeneous enhancement patterns (54.5%). Due to the small number of benign lesions, statistical comparisons between the malignant and benign groups were limited.

Conclusion: Breast MRI, particularly for BI-RADS 5 lesions, plays a critical role in the detection and characterization of breast cancer. The detailed assessment of morphological and dynamic features by MRI aids in accurate diagnosis and treatment planning. Understanding these MRI findings will enhance clinical decision-making and reduce unnecessary surgical interventions in patients with suspicious breast lesions.

Keywords: Breast cancer, magnetic resonance imaging, BI-RADS 5, lesion characterization, dynamic contrast-enhanced MRI

Introduction

Breast cancer remains the most frequently diagnosed cancer among women; therefore, early detection and accurate treatment determination are of vital importance.[1] Identification of early-stage breast cancer extends patient survival and improves response to treatment. Among breast imaging methods, magnetic resonance imaging (MRI) is increasingly used to diagnose breast lesions and determine treatment approaches.[1,2] It holds significant value, especially for high-risk patient groups and individuals with dense breast tissue, because it provides a more sensitive and detailed examination.[3]

Breast MRI is advantageous in diagnosing early-stage malignancies because it can reveal abnormalities that standard procedures like mammography and ultrasonography, might not be able to identify. MRI also assesses the dynamic and kinetic characteristics of breast lesions, along with providing detailed information about the size, location, and relationship of the tumor with the surrounding tissues.[1,4] This information is crucial in surgical planning, particularly in defining tumor boundaries and detecting multifocal or multicentric disease. Furthermore, MRI can be used to assess the effectiveness of the treatment process by monitoring the response to neoadjuvant chemotherapy. Another important application is the detection of occult breast cancer. Given these contributions, breast MRI has become an indispensable component of modern breast imaging practices.

The Breast Imaging-Reporting and Data System (BI-RADS) atlas defines the BI-RADS 5 category as highly suspicious lesions with a probability of malignancy exceeding 95%. In MRI, these lesions typically appear as masses with irregular or spiculated margins, heterogeneous internal structures, and rapid contrast uptake. Accurate assessment of lesions exhibiting mass enhancement is vital for distinguishing between malignancy and benignity. Parameters such as shape and margin characteristics, enhancement homogeneity, presence of septa, and enhancement kinetics should be evaluated together for a more accurate diagnosis.[4-6]

Non-mass enhancements on MRI are classified as focal, linear, ductal, segmental, regional, and multiple regional. The segmental-type

Cite this article as: Coşgun Z, Dağıstan E. Retrospective Evaluation of Magnetic Resonance Imaging Findings for BI-RADS 5 Lesions: A 5-year Clinical Experience. Adv Radiol Imaging. 2024;1(2):28-32

Address for Correspondence: Zeliha Coşgun MD, Bolu Abant İzzet Baysal University Faculty of Medicine, Department of Radiology, Bolu, Turkey
Phone: +90 541 828 33 45 **E-mail:** zeliha44@gmail.com **ORCID ID:** orcid.org/0000-0003-1996-1568
Received: 27.06.2024 **Accepted:** 19.07.2024

enhancement pattern is generally interpreted as BI-RADS 5, whereas the category of other non-mass enhancement patterns is determined by considering signal characteristics, diffusion properties, and enhancement features.[5]

BI-RADS 5 lesions often exhibit a washout pattern on dynamic contrast-enhanced imaging. This kinetic characteristic is considered an indicator of angiogenesis specific to malignancies. Additionally, BI-RADS 5 lesions may show signs of invasion into surrounding tissues and exhibit multifocal or multicentric features. These characteristics, which clearly reveal the relationship and spread of the tumor with surrounding structures, are critical in determining surgical planning and treatment strategies. The detailed imaging capability of MRI facilitates the accurate and timely diagnosis of lesions with a high probability of malignancy.[1,4]

Rapid assessment and histopathological examination of BI-RADS 5 lesions are necessary. However, benign pathological results can sometimes be obtained in the BI-RADS 5 category. Surgical excision is required in cases of radiopathological discordance. To reduce unnecessary surgical excisions, better characterization of findings with a high probability of malignancy on MRI is important.

The aim of this study was to examine the morphological and dynamic characteristics of the BI-RADS 5 category on MRI and to identify the most robust MRI findings for malignancy.

Methods

This study was approved by the Medical Research Ethics Committee of Bolu Abant University Faculty of Medicine (decision no: 2024:144, date: 25.03.2024). Informed consent was obtained from all patients prior to MRI. Given that the study was conducted retrospectively, no additional approval was required. Breast MRI scans performed between January 2019 and December 2023, which were reported as BI-RADS 5 lesions, underwent retrospective review using a picture archiving and communication system. The study included 120 patients who underwent biopsy or surgical excision. Radiological images were retrospectively evaluated by two radiologists with 16 and 9 years of experience in breast radiology who were blinded to the pathological diagnosis. The lesion characteristics were reported based on consensus agreement.

MRI was performed using the General Electric Signa™ Explorer MR 1.5T closed system device (GE Healthcare, Chicago, Illinois, IL, United States). Patients were positioned prone, and their breast tissues were positioned within a dedicated surface breast coil. MRIs were obtained using axial, fat-suppressed, and fast spin-echo T2-weighted imaging sequences, along with pre-contrast and post-contrast dynamic axial T1-weighted three-dimensional, fat-suppressed, fat-spoiled gradient-echo sequences. During the MRI examinations, a comprehensive assessment and documentation of various parameters, such as breast parenchymal structure, signal characteristics of lesions on T2-weighted images, as well as lesion size, location, enhancement type, shape, margins, enhancement patterns, and kinetic curve type on dynamic contrast-enhanced images, were performed.

Histopathological results for lesions that underwent biopsy or surgical excision were obtained from the hospital information system.

Statistical Analysis

Statistical software (Statistical Package for the Social Sciences 18 for Windows, IBM Co, Chicago, IL, USA) was used for statistical analyses. Kolmogorov-Smirnov test was applied to the study variables for normality analysis. Variables that fit into normal distribution were determined using one-way ANOVA and expressed as means and standard deviations. Other variables that did not fit the normal distribution were expressed as medians (minimum-maximum) and compared using the Kruskal-Wallis test. Categorical variables were compared between study groups using the chi-square test and presented as numbers and percentages. The correlation between study variables was analyzed using Pearson's correlation coefficient.

Results

In our study, a total of 120 BI-RADS 5 lesions were included, including 109 malignant and 11 benign lesions. The median age of patients with malignant lesions was 51 years (32-77), whereas the median age of patients with benign lesions was 52 years (20-78).

Out of the 109 patients diagnosed with malignant lesions, the breast parenchymal pattern was categorized as follows: 10 patients (9.2%) had type A, 27 patients (24.8%) had type B, 36 patients (33%) had type C, and 36 patients (33%) had type D. Out of the 11 patients diagnosed with benign lesions, the breast parenchymal pattern was categorized as follows: 1 patient (9.1%) had type A, 2 patients (18.2%) had type B, 2 patients (18.2%) had type C, and 6 patients (54.5%) had type D. Comparison between the two groups could not be performed due to the small number of benign lesions.

Basal enhancement was observed in a total of 109 patients with malignant lesions, with minimal enhancement in 2 patients (1.8%), mild enhancement in 49 patients (45%), moderate enhancement in 33 patients (30.3%), and marked enhancement in 25 patients (22.9%). Among patients with benign lesions, basal enhancement was mild in 3 patients (27.3%), moderate in 5 patients (45.4%), and marked in 3 patients (27.3%).

In malignant patients, 61 lesions (56%) appeared hypointense and isointense, and 48 lesions (44%) appeared hyperintense on T2-weighted images. In benign lesions, 4 lesions (36.4%) were hypointense, while 7 lesions (63.6%) were hyperintense on T2-weighted signals.

In malignant lesions, 1 lesion (0.9%) exhibited a focus, 9 lesions (8.3%) showed nonmass enhancement, and 99 lesions (90.8%) were in a mass configuration. In benign lesions, 9 (81.8%) were mass lesions, whereas 2 (18.2%) were nonmass-enhancing lesions.

In malignant lesions, 2 (1.96%) exhibited persistent enhancement, 16 (15.7%) exhibited plateau enhancement, and 84 (82.3%) demonstrated washout enhancement. The kinetic curve did not optimally evaluate in 7 non-mass enhancement observed in malignant lesions. In benign lesions, 3 (27.3%) showed persistent enhancement, 3 (27.3%) exhibited plateau enhancement, and 5 (45.5%) demonstrated washout enhancement.

Out of 100 malignant lesions with a mass configuration, 9 were round (9%), 34 were oval (34%), and 4 were lobulated (4%), while 53 were irregular in shape (53%). For benign lesions with a mass configuration, out of 9 lesions, 3 were oval (33.3%), 2 were lobulated (22.2%), and 4 were irregular in shape (44.4%).

Of the malignant lesions with mass enhancement, 13 (11.9%) were homogeneously enhancing, 76 (69.7%) were heterogeneously enhancing, 1 (0.9%) showed dark internal septations, and 10 (9.2%) exhibited rim enhancement. For benign lesions, 2 (18.2%) were homogeneously

enhancing, 6 (54.5%) were heterogeneously enhanced, and 1 (9.1%) had rim enhancement.

In malignant lesions, 1 lesion (10%) exhibited focal enhancement, 7 lesions (70%) showed segmental non-mass enhancement, and 2 lesions (20%) exhibited regional non-mass enhancement. For benign lesions, 1 lesion (50%) exhibited segmental non-mass enhancement and 1 lesion (50%) exhibited regional non-mass enhancement. The MRI findings are summarized in Table 1.

The pathological types and percentages of the 109 malignant lesions identified in this study are as follows: invasive lobular carcinoma accounted for 8.3%, tubular carcinoma for 2.8%, mucinous carcinoma for 0.9%, and infiltrating ductal carcinoma for the majority (Figures 1, 2), constituting 88.0% of the cases. These findings underscore the predominance of infiltrating ductal carcinoma among the malignant lesions studied, highlighting its significant presence in the cohort. The distribution of these pathological types provides valuable insights into the breast cancer subtype spectrum observed in the analyzed population. Among the identified benign lesions, there were 2 cases of fat necrosis (14.3%), 1 case of granulomatous mastitis (7.1%), 2 cases of fibrocystic changes (14.3%), 1 case of benign phyllodes tumor (7.1%) (Figure 3), 3 cases of fibroadenoma (21.4%), 1 case of radial scar (7.1%), and 1 case of intraductal papillomatosis (7.1%) (Figure 4). Inter-group

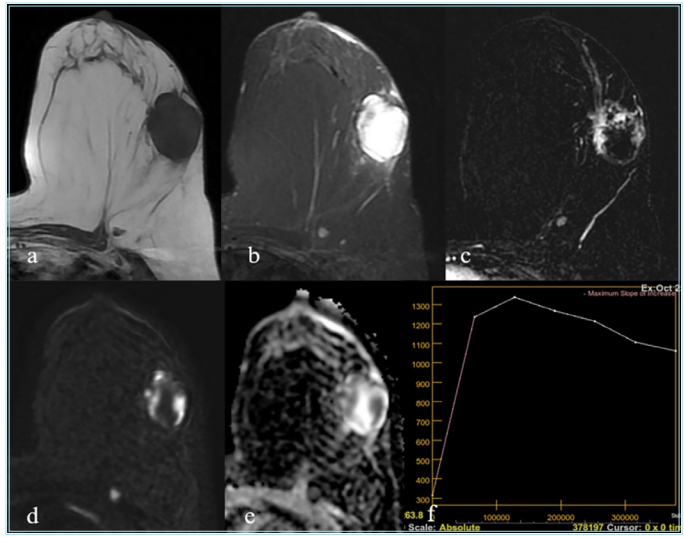

Figure 1. A 49-year-old female patient presented with a palpable mass. The mass appeared hypointense on T1-weighted imaging (a) and hyperintense on T2-weighted imaging (b), with lobulated contours and an oval shape. There is diffusion restriction in DWI (d, e), and the mass shows peripheral enhancement (c) and washout in the dynamic series (f). Histopathological diagnosis of invasive ductal carcinoma

Table 1. Magnetic resonance imaging findings

		Malignant lesions n (%)	Benign lesions n (%)
The breast parenchymal pattern (n=120)	A	10 (9.2)	1 (9.1)
	B	27 (24.8)	2 (18.2)
	C	36 (33)	2 (18.2)
	D	36 (33)	6 (54.5)
Basal enhancement (n=120)	Minimal	2 (1.8)	3 (27.3)
	Mild	49 (45)	0
	Moderate	33 (30.3)	5 (45.4)
	Marked	25 (22.9)	3 (27.3)
T2 signal characteristics (n=120)	Hypointense and isointense words	61 (56)	4 (36.4)
	Hyperintense	48 (44)	7 (63.6)
Lesion type (n=120)	Focus	1 (0.9)	0
	Non-mass enhancement	9 (8.3)	2 (18.2)
	Mass configuration	99 (90.8)	9 (81.8)
Kinetic curve type (n=113)	Persistent	2 (1.96)	3 (27.3)
	Plateau	16 (15.7)	3 (27.3)
	Washout	84 (82.3)	5 (45.5)
Mass shape (n=109)	Round	9 (9)	0
	Oval	34 (34)	3 (33.3)
	Lobulated	4 (4)	2 (22.2)
	Irregular	53 (53)	4 (44.4)
Mass enhancement (n=109)	Homogeneously	13 (11.9)	2 (18.2)
	Heterogeneously	76 (69.7)	6 (54.5)
	Dark internal septa	1 (0.9)	
	Rim	10 (9.2)	1 (9.1)
Non-mass distrubition (n=12)	Segmental	7 (70)	1 (50)
	Regional	2 (20)	1 (50)
	Focal	1 (10)	0

comparison could not be statistically performed because of the low number of benign lesions.

Discussion

MRI has significant advantages in breast imaging because of its high soft-tissue resolution for morphological assessment and dynamic evaluation capabilities, which help determine pathological features associated with tumor angiogenesis.[4] In our study, most malignant lesions exhibited heterogeneous enhancement patterns and were typically hypointense on T2-weighted signals. Specifically, 56% of the malignant lesions appeared hypointense and 44% appeared hyperintense on T2-weighted signals. This finding reflects differences in water content and cellular density in malignant lesions. In benign lesions, higher rates of hyperintense structures were observed on T2-weighted signals.[5]

A washout pattern was observed in 82.3% of malignant lesions, indicating angiogenesis specific to malignancy and rapid proliferation of tumor cells. In contrast, benign lesions more commonly exhibited homogeneous enhancement patterns. Notably, the washout kinetic model observed in many malignant lesions has been identified as an important indicator for assessing malignancy potential.[7] Our findings are consistent with the characteristic differences between malignant and benign lesions reported in the literature.[5,8]

It was found that the majority of malignant lesions had a mass configuration, with 53% having an irregular shape. This finding reflects the invasive and aggressive nature of malignant lesions, which is consistent with the literature.[2]

Our findings highlight the critical role of MRI in the early diagnosis of breast cancer and in determining appropriate treatment. It was

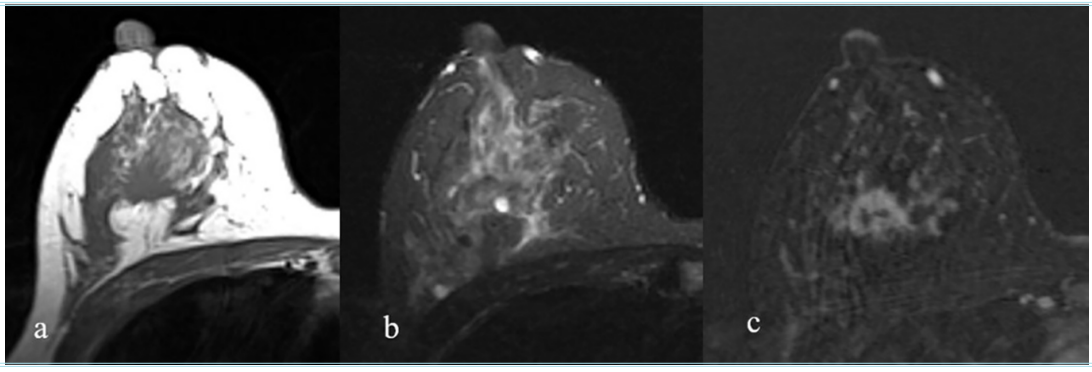

Figure 2. A 43-year-old female patient presented with a palpable mass. The mass appeared hypointense on both T1-weighted and T2-weighted magnetic resonance imaging images (a, b) and showed ring enhancement with spiculated contours on post-contrast images (c). Histopathological diagnosis of invasive ductal carcinoma

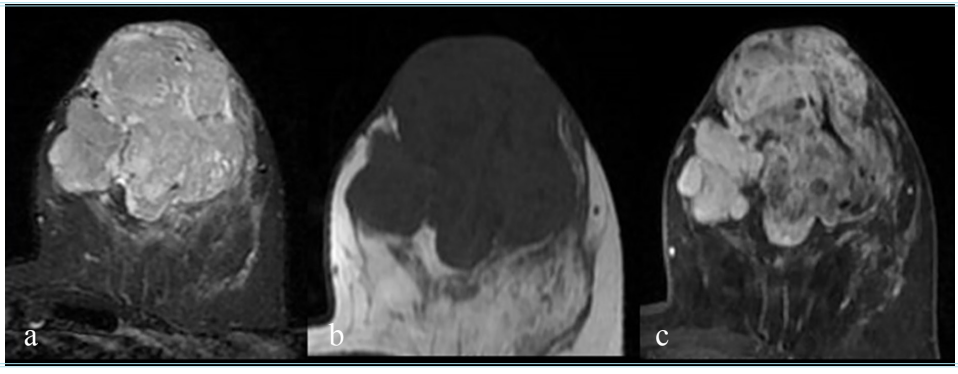

Figure 3. A 40-year-old patient presented with an 8-cm palpable mass in the left breast that caused nipple retraction and skin thickening. The mass appears hypointense on STIR sequence (a), hypointense on T1-weighted imaging (b), and shows heterogeneous enhancement on post-contrast images (c). Histopathologically, the lesion was a low-grade phyllode tumor

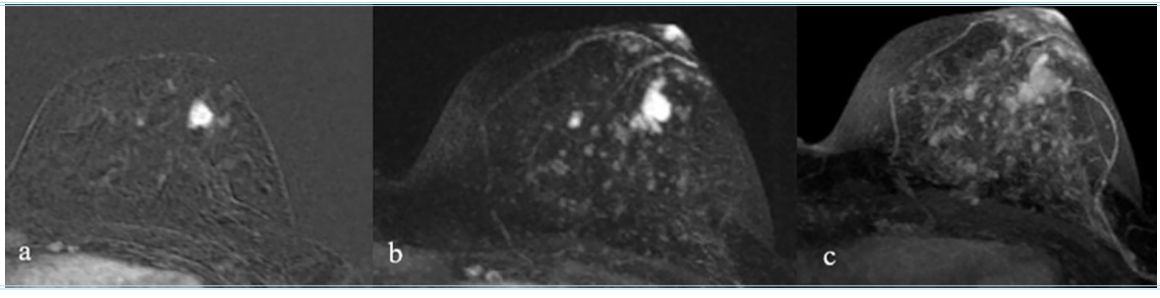

Figure 4. A 45-year-old female patient presented with an irregularly shaped, homogeneously enhancing solid lesion on post-contrast images (a). Dynamic imaging shows washout in both early and late phase MIP images (b, c). Histopathological diagnosis was intraductal papilloma

observed that the majority of lesions classified under BI-RADS 5 were malignant, and their morphological and dynamic characteristics were instrumental in diagnosis.[1,4,9]

Study Limitations

The main limitation of our study was the relatively small number of benign lesions included in the analysis. This limitation restricted our ability to perform robust statistical comparisons between benign and malignant BI-RADS 5 lesions. Future studies with larger sample sizes of benign lesions are needed to provide more definitive results.

Conclusion

In conclusion, the high-resolution images and dynamic contrast-enhanced examination methods offered by MRI have once again proven to be crucial tools for accurately classifying lesions and for surgical planning. These findings support the broader and standardized use of MRI in clinical practice. Future larger-scale studies will further validate the diagnostic accuracy and clinical utility of MRI.

Ethics

Ethics Committee Approval: This study was approved by the Medical Research Ethics Committee of Bolu Abant University Faculty of Medicine (decision no: 2024:144, date: 25.03.2024).

Informed Consent: Since the study was a retrospective study, informed consent was not required by the ethics committee.

Authorship Contributions

Surgical and Medical Practices: Z.C., E.D., Concept: Z.C., E.D., Design: Z.C., E.D., Data Collection or Processing: Z.C., Analysis or Interpretation: Z.C., Literature Search: Z.C., Writing: Z.C., E.D.

Conflict of Interest: No conflict of interest was declared by the authors.

Financial Disclosure: The authors declared that this study received no financial support.

References

1. Morris EA. Diagnostic breast MR imaging: current status and future directions. Radiol Clin North Am. 2007;45:863-80.
2. Liberman L. Clinical management issues in percutaneous core breast biopsy. Radiol Clin North Am. 2000;38:791-807.
3. Ding W, Fan Z, Xu Y, et al. Magnetic resonance imaging in screening women at high risk of breast cancer: A meta-analysis. Medicine (Baltimore). 2023;102:e33146.
4. Kuhl C. The current status of breast MR imaging. Part I. Choice of technique, image interpretation, diagnostic accuracy, and transfer to clinical practice. Radiology. 2007;244:356-78.
5. Schnall MD, Blume J, Bluemke DA, et al. Diagnostic architectural and dynamic features at breast MR imaging: multicenter study. Radiology. 2006;238:42-53.
6. Mann RM, Hoogeveen YL, Blickman JG, Boetes C. MRI compared to conventional diagnostic work-up in the detection and evaluation of invasive lobular carcinoma of the breast: a review of existing literature. Breast Cancer Res Treat. 2008;107:1-14.
7. Fischer U, Zachariae O, Baum F, von Heyden D, Funke M, Liersch T. The influence of preoperative MRI of the breasts on recurrence rate in patients with breast cancer. Eur Radiol. 2004;14:1725-31.
8. Bluemke DA, Gatsonis CA, Chen MH, et al. Magnetic resonance imaging of the breast prior to biopsy. JAMA. 2004;292:2735-42.
9. Orel S. Who should have breast magnetic resonance imaging evaluation? J Clin Oncol. 2008;26:703-11.

RESEARCH ARTICLE

DOI: 10.4274/AdvRadiolImaging.galenos.2024.22931
Adv Radiol Imaging 2024;1(2):33-6

Massively Invasive Ductal Breast Cancer: Association Between Mammographic Features and the HER2-enriched Molecular Subtype

Hüseyin Aydemir

Erbaa State Hospital, Clinic of Radiology, Tokat, Turkey

Abstract

Objectives: This study aimed to determine whether there were differences in mammographic characteristics (mass size and margin of the mass) between the HER2-enriched and non-HER2-enriched molecular subtypes of breast cancer.

Methods: A total of 142 individuals with mammographically verified masses and histopathologically diagnosed invasive ductal breast cancer were detected (HER2-enriched: n=29; HER2 non-enriched: n=113). Mammographic features related to HER2 molecular subtype were analyzed. According to the TNM staging criteria, patients with masses on mammography were divided into ≤2 cm (T1) and >2 cm (T2 and T3) groups. The margin characteristics of the mass detected by mammography were divided into spiculated and nonspiculated groups.

Results: Histopathological sampling was performed on the lesions of 142 patients with breast cancer who had mass lesions associated with invasive ductal carcinoma on mammography; 29/142 (20.4%) were HER2-enriched and 113/142 (79.5%) were non-HER2-enriched. On univariate analysis; HER2-enriched molecular subtype rates were significantly higher in tumor size ≤2 cm [17/60 (28.3%)] than in those >2 cm [12/82 (14.6%)] (p=0.007) and HER2-enriched molecular subtype rates were significantly higher in nonspiculated lesions [20/61 (32.7%)] than in spiculated lesions [9/81 (11.1%)] (p<0.001). No significant associations were observed between patients age and HER2-subtypes.

Conclusion: Small tumor sizes and non-spiculated masses were more likely to be HER2 molecular subtype. This study presents a predictive model that combines tumor size and nonspiculated mass mammographic characteristics. This model has the potential to determine the HER2-enriched subtype of breast cancer before surgery.

Keywords: Mammography, invasive ductal breast cancer, human epidermal growth factor receptor subtypes

Introduction

Breast cancer is the primary cause of cancer-related mortality in women globally, as well as the second leading cause of cancer-related death in the United States.[1] A highly distinct tumor that contains multiple subgroups. Based on the immunohistochemical expression of hormone receptors, these subtypes are commonly divided into four categories: progesterone receptor-positive (PR+), human epidermal growth factor receptor 2-positive (HER2+), and estrogen receptor-positive (ER+), which is defined by the absence of expression of any of the aforementioned receptors triple-negative breast cancer.[2]

About 15-25% of breast cancers express human epidermal 2 HER2, and the status of this receptor is primarily important for selecting the best course of treatments.[3] Chemotherapy combined with dual HER2 blockage with lapatinib/trastuzumab or neoadjuvant trastuzumab appears to be particularly beneficial for HER2-enriched subtypes.[4] Breast cancer radiogenomics investigation identified relationships between genetic subgroups and imaging abnormalities.[5] On mammography, patients with HER2-enriched breast cancer were more likely to show up with a non-spiculated lump.[6]

Clinical studies have shown that mammography screening is associated with reduced breast cancer mortality. However, screening healthy individuals is also associated with undesirable effects, such as women with false-positive results being recalled for additional imaging. Advocates of more aggressive screening strategies aim to maximize the benefits of early detection, while advocates of less frequent screening aim to reduce false-positive assessments, anxiety, and costs for patients who will never develop breast cancer. The World Health Organization has recommended that mammography screening begin at age 40 in well-resourced settings.[7-9]

Cite this article as: Aydemir H. Massively Invasive Ductal Breast Cancer: Association Between Mammographic Features and the HER2-enriched Molecular Subtype. Adv Radiol Imaging. 2024;1(2):33-6

Address for Correspondence: Hüseyin Aydemir MD, Erbaa State Hospital, Clinic of Radiology, Tokat, Turkey
Phone: +90 544 334 76 26 **E-mail:** aydemir334@hotmail.com **ORCID ID:** orcid.org/0000-0002-5698-1560
Received: 14.07.2024 **Accepted:** 26.07.2024

The HER2-enriched molecular subtype determines the medications and treatment modalities are advised.[10] Sometimes sampling artifacts, tiny biopsy specimens, or inoperability make it impractical to obtain enough tissue for examination prior to therapy initiation. In this situation, our study will be useful for decision-making. As a result, we aimed to explore the relationships between the HER2-subtype and mammographic features.

Methods

Ethics committee approval was obtained from the Erzincan Binali Yıldırım University, Mengücek Gazi Training and Research Hospital Research Committee (number: 2023-9/3, session: 3, date: 09.03.2023) for this study, and the Helsinki principles were adhered to during the study. Because of the retrospective study design, no additional informed consent forms were obtained from the patients. Between January 2018 and January 2023, patients with histopathologically confirmed invasive ductal breast cancer were screened from the institutional database. A total of 142 patients with mass lesions on mammography were included in the study. Mammographic characteristics (mass size and margin of the mass) and histopathological information (HER2-enriched molecular subtype and non-HER2-enriched molecular subtype) of the patients were recorded. The study included patients of all ages.

A consensus was reached after two radiologists who were blinded to the histological characteristics evaluated the mammography images for this study. The margin characteristics of the mass detected in the patients mammography were divided into spiculated and nonspiculated groups based on previous studies.[6,11] Lesions with lines radiating from their edges are called spiculated masses. If the lesion margins were circumscribed, microlobulated, obscured or indistinct were called non-speculated.

According to the TNM staging criteria, patients with masses on mammography were divided into ≤2 cm (T1) and >2 cm (T2 and T3) groups.

The tumor pathology reports of the patients were reviewed. The pathology reports were recorded as HER2-enriched and non-HER2-enriched molecular subtypes.

Statistical Analysis

The chi-square test (using Statistical Package for the Social Sciences software, version 15.0) was used to evaluate the correlation of HER2-enriched molecular subtype status with age and pathologic characteristics. Differences between breast cancers with and without HER2-enriched molecular subtypes were determined using the chi-square test, as well as univariate and multivariate binary logistic regression analyses. P<0.05 was considered statistically significant.

Results

As a result of histopathological sampling of the lesions of 142 breast cancer patients who had mass lesions related to invasive ductal carcinoma on mammography; 29/142 (20.4%) were reported as HER2-enriched and 113/142 (79.5%) were reported as non-HER2-enriched.

On univariate analysis, HER2-enriched molecular subtype rates were significantly higher in tumor size ≤2 cm [17/60 (28.3%)] than in those >2 cm [12/82 (14.6%)] (p=0.007) (Table 1).

On univariate analysis, HER2-enriched molecular subtype rates were significantly higher in nonspiculated lesions [20/61 (32.7%)] than in spiculated lesions [9/81 (11.1%)] (p<0.001) (Table 2).

Our results showed that small tumor sizes and non-spiculated masses were more likely to be HER2 molecular subtype.

No significant associations were observed between patient age and HER2 subtype (Table 3).

Table 1. Association between tumor size and HER2 subtypes

Tumor size	Non-HER2 enriched n (%)	HER2 enriched n (%)	Whole population (n)	Chi-square p value
≤2 cm	43 (71.7%)	17 (28.3%)	60	0.007*
>2 cm	70 (85.4%)	12 (14.6%)	82	

HER: Human epidermal growth factor receptor, n: Number, %: Percentage, *: Statistical significance

Table 2. Association between mass margin and HER2 subtypes

Margin of mass	Non-HER2 enriched n (%)	HER2 enriched n (%)	Whole population (n)	Chi-square p value
Spiculated mass	72 (88.9%)	9 (11.1%)	81	<0.001*
Non-spiculated mass	41 (67.3%)	20 (32.7%)	61	

HER: Human epidermal growth factor receptor, n: Number, %: Percentage, *: Statistical significance

Table 3. Age distribution of the HER2 subtypes

Age	Non-HER2 enriched n (%)	HER2 enriched n (%)	Whole population (n)	Chi-square p value
<35	7 (87.5%)	1 (12.5%)	8	0.751
35-69	101 (78.9%)	27 (21.1%)	128	
≥70	5 (83.3%)	1 (16.7%)	6	

HER: Human epidermal growth factor receptor, n: Number, %: Percentages

Discussion

The molecular characterization of breast cancer has led to a better understanding of the disease. Anti-HER2-targeted medicines have greatly improved the HER2-subtype, which has been associated with poor prognosis in seminal studies on cancer genetics.[12] An analysis of prior data indicated that compared with female patients with HER2-negative breast cancer, those with HER2-positive breast cancer who were treated with trastuzumab had a markedly better prognosis.[13]

The spiculation of malignant breast lesions often occurs because of substantial desmoplastic response. This feature is commonly observed in invasive breast cancer during mammography and serves as a valuable criterion for the clinical identification of the disease.[6,14] Imaging studies have revealed that grade 1 and 2 breast cancers exhibit a stromal response characterized by a spiculated margin.[15] Mammographic features have the ability to visually represent the characteristics of the breast tumor phenotype without the need for invasive procedures.[16] Recent studies have shown that masses with a spiculated margin are more frequently observed in patients with luminal A subtype than in other subtypes.[17,18] In addition, Liu et al.[6] noted that breast tumors with HER2 overexpression do not have a spiculated margin although the exact reason remains unclear. Our study showed that the rates of the HER2-enriched molecular subtype were considerably greater in nonspiculated than in spiculated lesions.

No statistically significant correlation between HER2/neu expression and tumor growth has been shown in earlier research.[19-22] Nevertheless, our investigation revealed a notable increase in the prevalence of the HER2-enriched molecular subtype in tumors 2 cm compared with larger lesions. These findings are consistent with those of Nie et al.[4], Bhagat et al.[23], and Almasri and Hamad.[24]

Study Limitations

Our study has some limitations. This study did not include other mammographic characteristics, such as microcalcification. It is appreciated that HER2 overexpression was not observed in most invasive lobular carcinomas, and invasive lobular carcinomas were not included in the study. Our study is retrospective, and data were collected from a single center. On the other hand, the predictive value of mammographic features was modest.

Conclusion

In conclusion, this study presents a predictive model that combines tumor size and nonspiculated mass mammographic characteristics. This model has the potential to determine the HER2-enriched subtype of breast cancer before surgery. Our study indicated that the tumor size was 2 cm, and it was more probable for the nonspiculated mass to belong to the HER2 molecular subtype. Radiologists should purposely search for this mammography finding to inform referring clinicians of the presence of this feature.

Ethics

Ethics Committee Approval: Ethics committee approval was obtained from the Erzincan Binali Yıldırım University, Mengücek Gazi Training and Research Hospital Research Committee (number: 2023-9/3, session: 3, date: 09.03.2023) for this study, and the Helsinki principles were adhered to during the study.

Informed Consent: Because this was a retrospective study, informed consent was not required by the ethics committee.

Financial Disclosure: The author declared that this study received no financial support.

References

1. Trayes KP, Cokenakes SEH. Breast Cancer Treatment. Am Fam Physician. 2021;104:171-8.
2. Orrantia-Borunda E, Anchondo-Nuñez P, Acuña-Aguilar LE, Gómez-Valles FO, Ramírez-Valdespino CA. Subtypes of Breast Cancer. In: Mayrovitz HN, editor. Breast Cancer [Internet]. Brisbane (AU): Exon Publications; 2022 Aug 6. Chapter 3.
3. Vaz-Luis I, Winer EP, Lin NU. Human epidermal growth factor receptor-2-positive breast cancer: does estrogen receptor status define two distinct subtypes? Ann Oncol. 2013;24:283-91.
4. Nie Z, Wang J, Ji XC. Retracted: Microcalcification-associated breast cancer: HER2-enriched molecular subtype is associated with mammographic features. Br J Radiol. 2021:20170942.
5. An YY, Kim SH, Kang BJ, Park CS, Jung NY, Kim JY. Breast cancer in very young women (<30 years): Correlation of imaging features with clinicopathological features and immunohistochemical subtypes. Eur J Radiol. 2015;84:1894-902.
6. Liu S, Wu XD, Xu WJ, Lin Q, Liu XJ, Li Y. Is There a Correlation between the Presence of a Spiculated Mass on Mammogram and Luminal A Subtype Breast Cancer? Korean J Radiol. 2016;17:846-52.
7. Canelo-Aybar C, Ferreira DS, Ballesteros M, et al. Benefits and harms of breast cancer mammography screening for women at average risk of breast cancer: A systematic review for the European Commission Initiative on Breast Cancer. J Med Screen. 2021;28:389-404.
8. Yala A, Mikhael P, Strand F, et al. Toward robust mammography-based models for breast cancer risk. Sci Transl Med. 2021;13:eaba4373.
9. Hubbard RA, Kerlikowske K, Flowers CI, Yankaskas BC, Zhu W, Miglioretti DL. Cumulative probability of false-positive recall or biopsy recommendation after 10 years of screening mammography: a cohort study. Ann Intern Med. 2011;155:481-92.
10. Coates AS, Winer EP, Goldhirsch A, et al. Tailoring therapies--improving the management of early breast cancer: St Gallen International Expert Consensus on the Primary Therapy of Early Breast Cancer 2015. Ann Oncol. 2015;26:1533-46.
11. Gao B, Zhang H, Zhang S, et al. Mammographic and clinicopathological features of triple-negative breast cancer. Br J Radiol. 2014;87:20130496.
12. Perou CM, Sørlie T, Eisen MB, et al. Molecular portraits of human breast tumours. Nature. 2000;406:747-52.
13. Dawood S, Broglio K, Buzdar AU, Hortobagyi GN, Giordano SH. Prognosis of women with metastatic breast cancer by HER2 status and trastuzumab treatment: an institutional-based review. J Clin Oncol. 2010;28:92-8.
14. Gokalp G, Topal U, Yildirim N, Tolunay S. Malignant spiculated breast masses: dynamic contrast enhanced MR (DCE-MR) imaging enhancement characteristics and histopathological correlation. Eur J Radiol. 2012;81:203-8.
15. Ramirez-Galvana YA, Uribe-Martinez MC, Ponce-Camacho MA, Montemayor-Martinez A. Spiculated margin on ultrasound is associated with tumor grade and immunohistochemical profile in breast cancer. J Mex Fed Radiol Imaging. 2022;1:119-25.
16. Gutman DA, Dunn WD, Grossmann P, et al. Somatic mutations associated with MRI-derived volumetric features in glioblastoma. Neuroradiology. 2015;57:1227-37.
17. Tamaki K, Ishida T, Miyashita M, et al. Correlation between mammographic findings and corresponding histopathology: potential predictors for biological characteristics of breast diseases. Cancer Sci. 2011;102:2179-85.

18. Jiang L, Ma T, Moran MS, et al. Mammographic features are associated with clinicopathological characteristics in invasive breast cancer. Anticancer Res. 2011;31:2327-34.

19. Yadav R, Sen R, Chauhan P. ER, PR, HER2/NEU status and relation to clinicopathological factors in breast carcinoma. Int J Pharm Pharm Sci. 2016;8:287-90.

20. Ayadi L, Khabir A, Amouri H, et al. Correlation of HER-2 over-expression with clinico-pathological parameters in Tunisian breast carcinoma. World J Surg Oncol. 2008;6:112.

21. Prati R, Apple SK, He J, Gornbein JA, Chang HR. Histopathologic characteristics predicting HER-2/neu amplification in breast cancer. Breast J. 2005;11:433-9.

22. Ariga R, Zarif A, Korasick J, Reddy V, Siziopikou K, Gattuso P. Correlation of her-2/neu gene amplification with other prognostic and predictive factors in female breast carcinoma. Breast J. 2005;11:278-80.

23. Bhagat VM, Jha BM, Patel PR. Correlation of hormonal receptor and Her-2/neu expression in breast cancer: a study at tertiary care hospital in south Gujarat. National journal of medical research. 2012;2:295-8.

24. Almasri NM, Al Hamad M. Immunohistochemical evaluation of human epidermal growth factor receptor 2 and estrogen and progesterone receptors in breast carcinoma in Jordan. Breast Cancer Res. 2005;7:R598-604.

RESEARCH ARTICLE

DOI: 10.4274/AdvRadiolImaging.galenos.2024.66375
Adv Radiol Imaging 2024;1(2):37-40

Comparison of Breast Magnetic Resonance Imaging and Mammography Findings in Detecting Ductal Carcinoma *in situ* in Preoperative Evaluation

Mustafa Özer

Kırşehir Training and Research Hospital, Clinic of Radiology, Kırşehir, Turkey

Abstract

Objectives: Breast cancer is the most common type of cancer in women, imaging methods have an important role in diagnosis and treatment. Ductal carcinoma *in situ* (DCIS) accounts for approximately 30% of new breast cancer diagnoses. It was aimed to retrospectively compare the sensitivities of breast magnetic resonance imaging (MRI) and mammography (MG) in detecting lesions in DCIS patients and predicting pathological subgroups of the lesion in the preoperative period.

Methods: Preoperative MRI and MG examinations of 150 lesions diagnosed with DCIS, with an average age of 59 years, were evaluated retrospectively. In our study, the sensitivities of MRI and MG were evaluated by comparing them with pathological dimensions. In addition, lesions were divided into pathological subgroups and sensitivity comparisons were made between imaging methods.

Results: Of the 150 DCIS lesions, 30 (20%) were found solely with MG screening, 15 (10%) were found solely with MRI examination, and the remaining 105 (70%) patients had both MG and MRI detection. While the average size of DCIS was 1.55 cm in 135 mammograms, it was 2.10 cm in 120 MRI examinations. It was statistically significantly lower in MG ($p<0.05$). Compared to the histopathological size of 105 cases in which lesions were found to be common in both examinations, the accuracy of MRI and MG was 0.64 and 0.58, respectively. Data finds MRI more sensitive in detecting DCIS ($p<0.05$). Pathological examinations revealed high-grade DCIS in 35 patients (23%) and low- and intermediate-grade DCIS in 115 patients (77%). In the sensitivity comparison between pathological subgroups, no significant statistical difference was found between the two imaging methods ($p>0.05$).

Conclusion: MRI detects a slightly larger size than MG, it has a higher sensitivity in detecting DCIS in younger patient groups.

Keywords: Ductal carcinoma *in situ*, DCIS, magnetic resonance imaging, MRI, mammography

Introduction

Ductal carcinoma *in situ* (DCIS) is a preinvasive or noninvasive breast cancer characterized by the proliferation of ductal epithelial cells confined to the terminal ductal lobular unit.[1] DCIS accounts for approximately 30% of new breast cancer diagnoses.[2] DCIS is a highly varied set of lesions distinguished by genetic and molecular abnormalities, histopathologic characteristics, and biologic indicators, as well as a varying risk of development to invasive disease. Some DCIS lesions will develop into an aggressive invasive malignancy.[3]

It is known that the incidence of invasive cancer in previous separation DCIS is approximately 40%.[4] It may also expand 20% of all breast cancers.[5] Therefore, determining the localization and distribution of DCIS before the operation is very important in approaching the patient. Mammography (MG) is regarded as the primary approach for detecting microcalcifications in radiological treatment.[6] However, MG has relative limitations in detecting DCIS and assessing tumor size, as foci of noncalcified DCIS cannot be demonstrated in dense breasts, and it can sometimes be difficult to distinguish calcifications associated with benign histology from malignant calcifications. Failure to appropriately establish the mass boundaries in patients may result in relapse and recurrent treatments.[7]

The research has demonstrated that evaluating mass dimensions preoperatively with a magnetic resonance imaging (MRI) examination is highly beneficial. The same is true for people with DCIS, which has been shown to be more effective than MG. However, there is no standardized preoperative technique using MRI in DCIS patients.[7-10]

The aim of this study is to investigate the efficacy of pre-operative breast MRI in assessing DCIS size in contrast to histopathological size, as well as to compare the accuracy of MRI and MG.

Cite this article as: Özer M. Comparison of Breast Magnetic Resonance Imaging and Mammography Findings in Detecting Ductal Carcinoma in situ in Preoperative Evaluation. Adv Radiol Imaging. 2024;1(2):37-40

Address for Correspondence: Mustafa Özer MD, Kırşehir Training and Research Hospital, Clinic of Radiology, Kırşehir, Turkey
Phone: +90 543 497 49 72 **E-mail:** dr.mustafaozer@yahoo.com **ORCID ID:** orcid.org/0009-0002-0570-2936
Received: 02.07.2024 **Accepted:** 11.08.2024

Methods

The Institutional Review Board approved this retrospective study. The retrospective nature of the decision precluded informed consent.

For this study, ethics committee approval numbered 938/2021 dated 22.12.2021 was received from Ankara Training and Research Hospital Clinical Research Ethics Committee.

The reports of patients who underwent breast MRI in our hospital were retrospectively reviewed using the hospital information management system. Among these patients, those diagnosed with breast cancer were examined, and those diagnosed with DCIS were included in the study. During the specified period, 150 patients were diagnosed with DCIS, forming the study population.

For all patients over, MG exams were conducted using the conventional craniocaudal and mediolateral-oblique projections (Figure 1).

All patients underwent MRI after conventional examinations to ensure that there were no disruptions in treatment (Figure 2). A 1.5 T whole body imaging equipment (Signa Excite, GE Healthcare, Milwaukee, WI, USA) was used to perform the MRI exams. Using a four-channel breast coil, the patient's breast was hung during the prone scan. With fat suppression, transverse and sagittal plane MRIs were acquired. Pre-contrast sagittal acquisitions were carried out with a T2-weighted fast spin-echo sequence, and pre-contrast transverse acquisitions were carried out using a T1-weighted fast spin-echo sequence and transverse T2-weighted fast spin echo short tau inversion recovery (STIR) imaging. Echo array suppressing fat deposits. Pre- and post-contrast sagittal dynamic imaging, 3D multiphase, VIBRANT (flip angle 10°; minimum 2.4 msec echo duration; maximum 14.0 msec echo time).

Biopsy was recommended for all cases for definitive diagnosis and treatment planning of the patients. Biopsy examination was performed with sonography in 105 of 150 patients, while 45 patients were marked with a stereotaxic wire and mammography.

The fourth edition of the MG and MRI breast imaging reporting and data system (BI-RADS) categories was followed by a radiologist with seven years of expertise in breast imaging to assess the characteristics. In the MG examination, the presence of masses, microcalcifications, and parenchymal distortions were noted. In the examination, the shape, contour, density and microcalcification morphology of the lesion were evaluated. In breast MRI examination, parenchymal background contrast enhancement of fibroglandular tissues and the mass structure of the lesions were determined in the morphology of the lesions. The contrast enhancement pattern and distribution of those that did not have a mass structure were noted.

DCIS was categorized based on nuclear grade (high, intermediate, and low). Microinvasion is the term used to describe the unfocused spread of cancer cells into neighboring tissues via the basement barrier.

Statistical Analysis

The study data was analyzed using IBM Statistical Package for the Social Sciences (SPSS) Inc., Chicago, IL's SPSS for Windows 20. The normal distribution of the data was confirmed by the Kolmogorov-Smirnov test. For numerical data that is regularly distributed, the mean and standard deviation are shown. When displaying data that does not follow a normal distribution, the median is utilized. Both the Mann-Whitney U test and the Student's t-test were used to compare numerical variables between groups. Statistically significant value of $p<0.05$ was used.

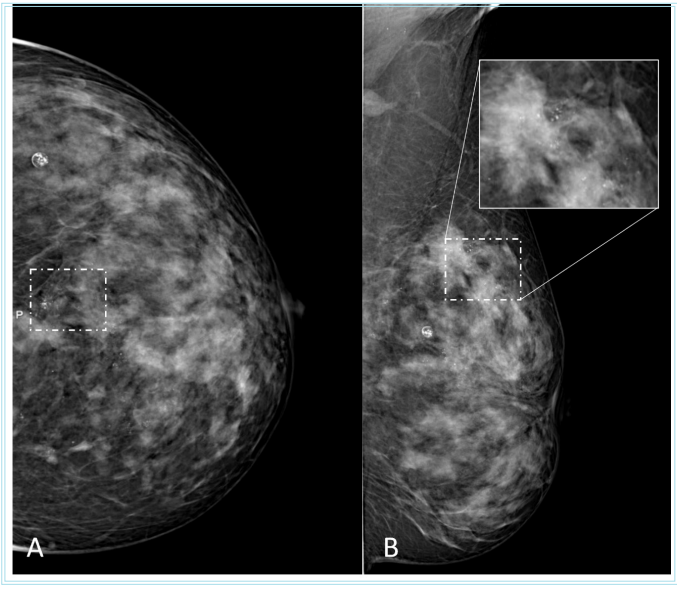

Figure 1. Mammography images of a 63-year-old female patient diagnosed with ductal carcinoma *in situ* (DCIS). A) In the craniocaudal view, pleomorphic calcifications clustered in the central area (rectangle) are observed. B) In the mediolateral oblique view, pleomorphic calcifications clustered in the upper zone (rectangle) are observed. The core biopsy from the defined area confirmed a diagnosis consistent with DCIS

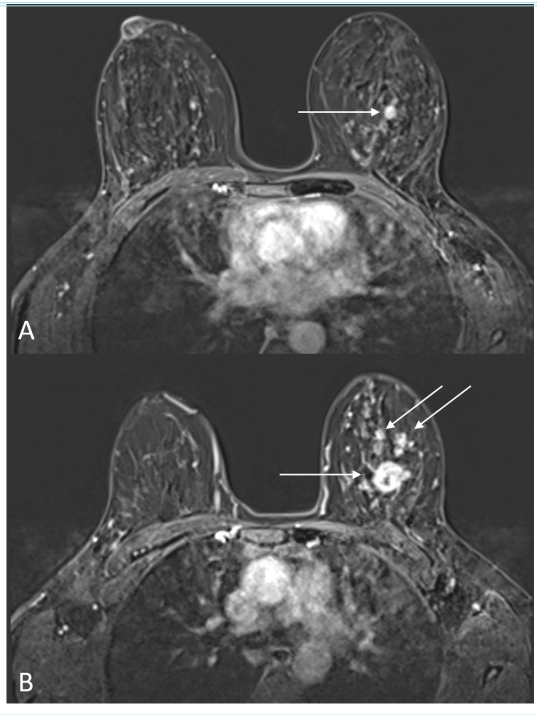

Figure 2. Contrast-enhanced breast magnetic resonance imaging images of a 63-year-old female patient diagnosed with ductal carcinoma *in situ* (DCIS). A) A subcentimetric enhancing solid lesion in the central area of the left breast is observed (arrow). B) In more superior sections, larger and multifocal enhancing lesions are observed in the same patient (arrows). The pathological results of these lesions were consistent with DCIS.

Results

Of the 150 DCIS lesions, 30 (20%) were found solely with MG screening, 15 (10%) were found solely with MRI examination, and the remaining 105 (70%) patients had both MG and MRI detection (10%, 20%, and 70%, respectively).

In the MG examination of 150 patients, type D pattern was observed in 15 (10%) patients, type C pattern was observed in 50 (33.3%) patients, type B pattern was observed in 50 (33.3%) patients, and type A pattern was observed in 35 (23.3%) patients. In the MG examination, there was a mass appearance in 25 (16%) of 150 patients, only microcalcification in 95 (63%), microcalcification along with the mass in 10 (7%) patients, and only parenchymal distortion in the remaining 20 (5%) patients.

Lesions could be visualized in a total of 120 (80%) MRI examinations. While contrast enhancement without mass effect was observed in 110 (73.3%) patients, MRI examination was observed as false negative in 10 (6.7%) patients.

While the average size of DCIS was 1.55 cm in 135 mammograms, it was 2.1 cm in 120 MRI examinations. It was statistically significantly lower in MG ($p< 0.05$).

In the pathological examinations, high-grade DCIS was observed in 35 (23%) patients, and low- and intermediate-grade DCIS was observed in 115 (77%) patients. There was no microinvasion in 135 (90%) of the patients. Seventy-four (49%) of the lesions were observed in the right breast and 76 (51%) were observed in the left breast.

Compared to the histopathological size of 105 cases in which lesions were found to be common in both examinations, the accuracy of MRI and MG was 0.64 and 0.58, respectively. MRI showed better accuracy than MG for younger patients. The current situation was found to be significant in terms of accuracy in the MRI examination ($p<0.05$). While no significant difference was observed in tumor nuclear staging in any group, it was slightly closer to significance in the middle group ($p=0.06$).

Discussion

In our study, we investigated the sensitivities of DCIS lesions in MG and MRI examinations. In our study, lesions were detected in MG examination in 135 (90%) patients and in MRI examination in 120 (80%) patients. In this case, unlike the study conducted by Kuhl et al.[11], MG examination was found to be more sensitive in detecting DCIS. However, in our study, while stereotaxic marking was used to guide pathological diagnosis, breast MRI vacuum biopsy method was not used. This may indicate that MG is falsely more sensitive.

In our study, microcalcification was detected in 63% of the lesions, while MRI contrast enhancement causing mass effect was observed in 73%. While the appearance showed a similar correlation with the literature in terms of microcalcification, the microcalcification rate was observed to be lower.[12,13] In our study, MG examination revealed a mass rate of 16%, microcalcification with a mass rate of 7%, and parenchymal distortion rate of 13%. These rates are higher than those in the literature.[14,15] In MRI examination, the contrast enhancement rate of the lesions was similar to the literature.[16,17]

Since DCIS is the early stages of the malignant process, tumor size may change the treatment process. In our study, MG was able to detect smaller lesions (2.1 cm versus 1.55 cm). When we look at the literature, we found that the average size of the lesions detected in MG examination was lower in the study by Kim et al.[18], similar to our study. This situation was evaluated due to the ability to detect calcification in MG examination of small lesions.

It is shown in the literature that MRI has a higher accuracy rate in detecting the lesion and showing its pathological extent.[11] In our study, the relationship between post-pathology size and detectable MRI and MG sizes was consistent with the literature.[19]

When the current sources in the literature were evaluated in comparison with the study by Proulx et al.[7], the number of lesions in our study was almost twice as high (150 lesions versus 79 lesions). Compared to the study of Proulx et al.[7], our MRI and MG lesion detectability rates were similar. However, contrary to the study conducted by Proulx et al.[7], in our study, the p values regarding MRI sensitivity in tumors diagnosed as middle-stage pathologically were not significant, although they were low. The current situation may be due to the lack of homogeneous distribution of the patient group in our study. As it is known, MRI examination is sensitive in the diagnosis of DCIS at early ages due to the low sensitivity of MG in the young group. For this purpose, the cut-off value can be determined in future studies in DCIS screening according to age.

Study Limitations

There are several limitations in our study. First, although our patient population was higher than in the literature, it was performed in a single center and evaluated retrospectively. Secondly, since subgroups for the patient population were not performed, the sensitivity of our study according to age was low. Thirdly, a single radiologist evaluated the examinations. This may have caused bias in the results. Fourth, since there is no MRI vacuum biopsy technique in our center, this may have affected the results.

Conclusion

Although MRI detects a slightly larger size than MG, it has a higher sensitivity in detecting DCIS in younger patient groups.

Ethics

Ethics Committee Approval: For this study, ethics committee approval numbered 938/2021 dated 22.12.2021 was received from Ankara Training and Research Hospital Clinical Research Ethics Committee.

Informed Consent: Since the study was a retrospective study, informed consent was not required by the ethics committee.

Financial Disclosure: The author declared that this study received no financial support.

References

1. Bijker N, Donker M, Wesseling J, den Heeten GJ, Rutgers EJ. Is DCIS breast cancer, and how do I treat it? Curr Treat Options Oncol. 2013;14:75-87.
2. Grimm LJ. Radiology for Ductal Carcinoma In Situ of the Breast: Updates on Invasive Cancer Progression and Active Monitoring. Korean J Radiol. 2024;25.
3. Greenwood HI, Wilmes LJ, Kelil T, Joe BN. Role of Breast MRI in the Evaluation and Detection of DCIS: Opportunities and Challenges. J Magn Reson Imaging. 2020;52:697-709.
4. Chootipongchaivat S, van Ravesteyn NT, Li X, et al. Modeling the natural history of ductal carcinoma in situ based on population data. Breast Cancer Res. 2020;22:53.

5. Pinder SE. Ductal carcinoma in situ (DCIS): pathological features, differential diagnosis, prognostic factors and specimen evaluation. Mod Pathol. 2010;23(Suppl 2):8-13.
6. Ernster VL, Ballard-Barbash R, Barlow WE, et al. Detection of ductal carcinoma in situ in women undergoing screening mammography. J Natl Cancer Inst. 2002;94:1546-54.
7. Proulx F, Correa JA, Ferré R, et al. Value of pre-operative breast MRI for the size assessment of ductal carcinoma in situ. Br J Radiol. 2016;89:20150543.
8. Burstein HJ, Polyak K, Wong JS, Lester SC, Kaelin CM. Ductal carcinoma in situ of the breast. N Engl J Med. 2004;350:1430-41.
9. EORTC Breast Cancer Cooperative Group; EORTC Radiotherapy Group; Bijker N, Meijnen P, Peterse JL, et al. Breast-conserving treatment with or without radiotherapy in ductal carcinoma-in-situ: ten-year results of European Organisation for Research and Treatment of Cancer randomized phase III trial 10853--a study by the EORTC Breast Cancer Cooperative Group and EORTC Radiotherapy Group. J Clin Oncol. 2006;24:3381-7.
10. Allegra CJ, Aberle DR, Ganschow P, et al. National Institutes of Health State-of-the-Science Conference statement: Diagnosis and Management of Ductal Carcinoma In Situ September 22-24, 2009. J Natl Cancer Inst. 2010;102:161-9.
11. Kuhl CK, Schrading S, Bieling HB, et al. MRI for diagnosis of pure ductal carcinoma in situ: a prospective observational study. Lancet. 2007;370:485-92.
12. Hofvind S, Iversen BF, Eriksen L, Styr BM, Kjellevold K, Kurz KD. Mammographic morphology and distribution of calcifications in ductal carcinoma in situ diagnosed in organized screening. Acta Radiol. 2011;52:481-7.
13. Greenwood HI, Heller SL, Kim S, Sigmund EE, Shaylor SD, Moy L. Ductal carcinoma in situ of the breasts: review of MR imaging features. Radiographics. 2013;33:1569-88.
14. Barreau B, de Mascarel I, Feuga C, et al. Mammography of ductal carcinoma in situ of the breast: review of 909 cases with radiographic-pathologic correlations. Eur J Radiol. 2005;54:55-61.
15. Stomper PC, Connolly JL, Meyer JE, Harris JR. Clinically occult ductal carcinoma in situ detected with mammography: analysis of 100 cases with radiologic-pathologic correlation. Radiology. 1989;172:235-41.
16. Shiraishi A, Kurosaki Y, Maehara T, Suzuki M, Kurosumi M. Extension of ductal carcinoma in situ: histopathological association with MR imaging and mammography. Magn Reson Med Sci. 2003;2:159-63.
17. Kim DY, Moon WK, Cho N, et al. MRI of the breast for the detection and assessment of the size of ductal carcinoma in situ. Korean J Radiol. 2007;8:32-9.
18. Kim DY, Moon WK, Cho N, et al. MRI of the breast for the detection and assessment of the size of ductal carcinoma in situ. Korean J Radiol. 2007;8:32-9.
19. Marcotte-Bloch C, Balu-Maestro C, Chamorey E, et al. MRI for the size assessment of pure ductal carcinoma in situ (DCIS): a prospective study of 33 patients. Eur J Radiol. 2011;77:462-67.

RESEARCH ARTICLE

DOI: 10.4274/AdvRadiolImaging.galenos.2024.35229
Adv Radiol Imaging 2024;1(2):41-5

Significance of Shear Wave Elastography and B-Mode Ultrasound in Assessing Axillary Lymph Nodes in Patients with Breast Cancer

Cansu Öztürk

Atatürk Sanatoryum Training and Research Hospital, Clinic of Radiology, Ankara, Turkey

Abstract

Objectives: The purpose of this study was to investigate the potential benefits of including shear wave elastography (SWE) testing alongside B-Mode ultrasonography (US) in identifying morphologic abnormalities in individuals diagnosed with breast cancer involving axillary lymph nodes (ALNs).

Methods: Fifty-seven patients with breast cancer whose ALN spread was investigated were included in this study. Lymph nodes were evaluated using B-Mode US to determine cortical thickness, absence of fatty hilum, presence of a non-hilar blood supply, and a long axis to short axis ratio greater than two. The same patients were evaluated using SWE. Following the assessment of SWE, a core biopsy of the lymph nodes was performed using US guidance.

Results: A biopsy was performed in 57 patients. A total of 45 patients exhibited lymph node metastases, whereas the remaining 12 patients exhibited reactive lymph node hyperplasia. The Emax of the cortex exhibited a higher degree of specificity than the cortical thickness (81.8% vs. 72.7%). The specificity was found to be equal (90.9%) between the combination of Emax of the cortex and cortical thickness, as well as between at least two B-Mode US characteristics.

Conclusion: In conclusion, SWE is valuable for distinguishing between metastases and reactive hyperplasia in individuals exhibiting suspicious features on B-Mode US of ALNs.

Keywords: Shear wave elastography, SWE, elastography, sonography, breast cancer, axillary lymph nodes

Introduction

Breast cancer is a prevalent form of cancer among women worldwide and is the leading cause of cancer-associated mortality.[1] The evaluation of recurrences and metastases is frequently conducted through the investigation of axillary lymph nodes (ALNs).[2] The evaluation of ALN has significant predictive value in the context of breast cancer. The preoperative ALN status is a crucial benchmark for clinical staging and the formulation of treatment strategies for breast cancer.[3,4]

Ultrasonography (US) is currently the imaging technique of choice for evaluating the axilla.[5] In ALN, the presence of a round ALN, a long-axis-to-short-axis ratio of 2, cortical thickness of >3 mm, and an obliterated fatty hilus are indicative of metastatic ALNs.[6] Axillary US has a sensitivity ranging from 35% to 82% and specificity ranging from 73% to 97.9%.[7,8] Despite being an invasive procedure, US-guided core needle biopsy has demonstrated remarkable sensitivity and specificity for detecting metastases.[9,10] Due to the invasive nature of biopsy, a non-invasive imaging examination is required to predict the presence of metastatic ALNs.

US, a non-invasive modality referred to as elastography, can yield significant insights into the stiffness properties of lesions.[11,12] US elastography has the capability to objectively evaluate variations in stiffness between benign and malignant lymph nodes.[13,14] Shear wave elastography (SWE) has been the subject of numerous studies. Recent elastographic investigations examining ALNs have revealed that the precision of subcutaneous US may exhibit variability as a result of anatomical irregularities inside the axillary cavity, the deep positioning of the lymph node, and the reliance on the technique by the user.[15] Nevertheless, there is a scarcity of research on the identification of metastatic ALNs in individuals diagnosed with breast cancer.[16] Chang et al.[17] found that although SWE has limited sensitivity in the evaluation of ALNs, the simultaneous application of US and SWE was useful for lymph node evaluation. The determinant is the cortical thickening of the lymph nodes. Both benign reactive hyperplasia and nodal metastases often show cortical thickening on US. Several studies have been conducted to compare the diagnostic efficacy of SWE techniques with B-Mode US features.[16-19] Nevertheless, metastatic lymph nodes frequently have dubious morphological characteristics. Hence, it is our contention that the integration of SWE with B-Mode US characteristics

Cite this article as: Öztürk C. Significance of Shear Wave Elastography and B-Mode Ultrasound in Assessing Axillary Lymph Nodes in Patients with Breast Cancer. Adv Radiol Imaging. 2024;1(2):41-5

Address for Correspondence: Cansu Öztürk MD, Atatürk Sanatoryum Training and Research Hospital, Clinic of Radiology, Ankara, Turkey
Phone: +90 505 269 00 73 **E-mail:** cnsozt@yahoo.com **ORCID ID:** orcid.org/0000-0003-3659-5184
Received: 30.05.2024 **Accepted:** 11.08.2024

can provide advantageous outcomes in real-world applications. The primary objective of this study was to investigate the potential benefits of including SWE testing alongside B-Mode US for identifying morphologic abnormalities in individuals diagnosed with breast cancer involving ALNs.

Methods

The Erzincan Binali Yıldırım University Clinical Researches Ethics Committee, 16.05.2024, EBYU KAEK 2024.05-1.2356093-113. approved the study, and informed consent was obtained. The study was initiated after obtaining written informed consent from the patients.

Study Population

The research was carried out prospectively. The study comprised individuals who were diagnosed with breast cancer by fine needle aspiration biopsy and those with suspicious ALNs on US. The study omitted ALNs that were anatomically deep and suspected of metastasis due to the absence of a clear evaluation in SWE. Furthermore, those diagnosed with ALN-producing conditions of non-malignant nature, such as granulomatous or lymphoproliferative diseases, were not included in the study. In total, 65 patients with breast cancer were assessed for potential metastases in the lymph nodes using axillary US-guided biopsy. Of the 65 patients, eight were excluded from the study because their lymph nodes were located at a deep anatomical level. Consequently, the study incorporated the remaining 57 individuals for the purpose of ALN examination.

B-Mode US

All patients were evaluated by a radiology physician with 15 years of experience in breast radiology using a 3.5- or 5-MHz real-time US device (Samsung RS85 Prestige, South Korea). Lymph nodes at the axillary level with diffuse cortex thickening or asymmetrical lymph nodes up to 3 mm in thickness were considered suspicious for metastasis. Lymph nodes with increased cortical thickness (>6.7 mm) were selected for B-Mode US-guided evaluation. Lymph nodes were evaluated using B-Mode US to determine cortical thickness, absence of fatty hilum, presence of a non-hilar blood supply, and a long axis to short axis ratio greater than 2.

Shear Wave Elastography

The same patients were evaluated using SWE. localization of the lymph nodes was observed in the central region of the SWE window (Figures 1, 2). The probe remained stationary until the color maps reached a state of stability and photographs were obtained. the typical range of the elastography map was reduced from 180 kPa until more challenging regions within the lymph node became visible. Quantitative SWE features were placed in the hardest regions of the cortex and hilus. A region of interest (ROI) of 1 mm was used to analyze several non-overlapping lymph nodes characterized by a thin cortex

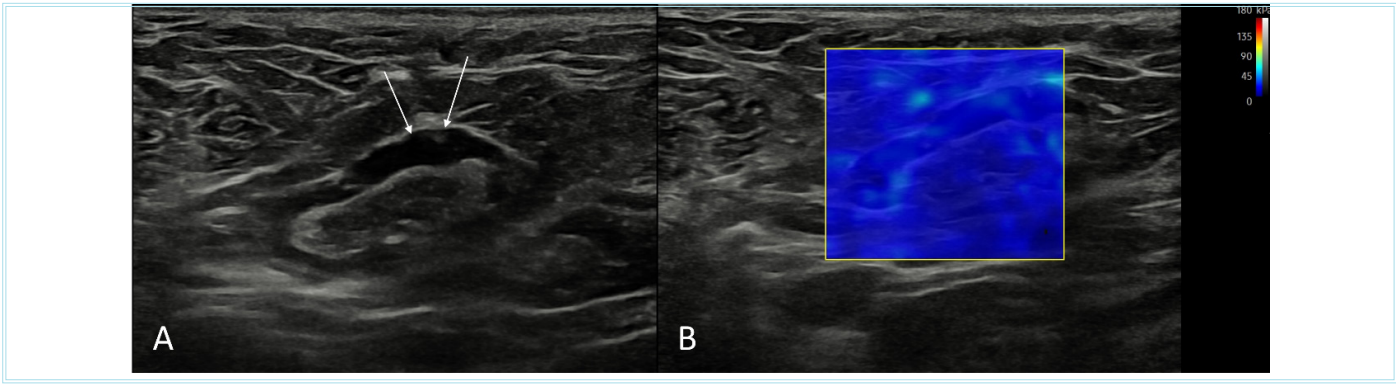

Figure 1. A 57-year-old female patient diagnosed with breast cancer. A) B-Mode ultrasound image of the right axillary lymph node showing focal mild cortical thickening (arrows) is present. B) Shear wave elastography image of the same lymph node showing no color coding indicative of tissue stiffening is observed (rectangle). Core biopsy pathological findings indicated a reactive lymph node. Elastographic measurement values are not numerically presented in this figure

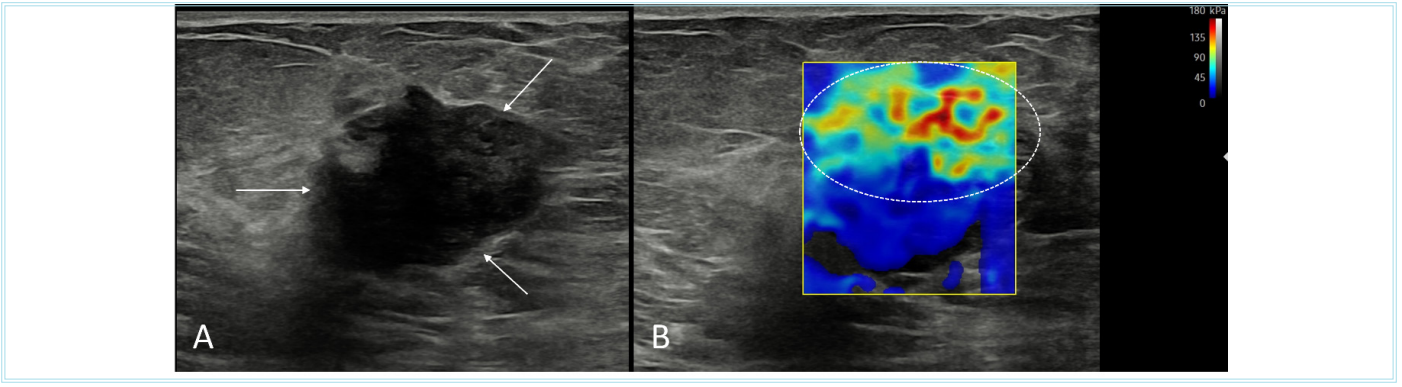

Figure 2. A 54-year-old female patient diagnosed with breast cancer and axillary metastasis. A) In the B-Mode ultrasound image of the left axillary pathological lymphadenopathy (arrows), findings include diffuse thickening of the cortex, absence of the fatty hilum, and a long-axis to short-axis ratio greater than two. B) In the shear wave elastography image of the same pathological lymph node, color coding indicative of tissue stiffening is observed (circle). Elastographic measurement values are not numerically presented in this figure

and clear hilus. Three ROI values were created using this method, and the parameter with the highest reading was selected. The parameters Emax (highest elasticity value), Emin (lowest elasticity value), Emean (average elasticity value), and ESD (standard deviation of elasticity) were evaluated in this study.

Biopsy

Following the assessment of SWE, a core biopsy of the lymph nodes was performed using US guidance. Pathological findings from the biopsied lymph nodes were utilized as a benchmark to assess the diagnostic efficacy of B-Mode US and SWE. In this investigation, the pathologist was unaware of the evaluation outcomes of B-Mode US and SWE.

Statistical Analysis

For data analysis, Statistical Package for the Social Sciences version 20.0 for Windows was used. The normality of the data distribution was assessed using the Kolmogorov-Smirnov test. Categorical variables were evaluated using the chi-square test, whereas parametric variables were analyzed using the Mann-Whitney U test. Additionally, receiver operating characteristics analysis was conducted to determine the sensitivity and specificity. In all evaluations, a p value 0.05 was considered statistically significant.

Results

Table 1 presents the demographic and clinical characteristics of the 57 study patients. The mean age of the 57 patients was 48.1±10.1 years. One of these patients was male, and the others were female. Twenty-seven (47.4%) of the 57 patients were postmenopausal. Patients described a palpable breast mass that lasted a mean of 6.0±0.9 months when they visited the clinic. The upper outer quadrant was the most common site of breast mass in 33 (57.9%) of the 57 patients. It was also shown that the luminal subtype was the most common subtype, affecting 20 (35.1%) patients.

Axillary US and US-guided Biopsy

A total of 312 ALNs, all located on the same side, were identified as suspects of metastasis using axillary US in a cohort of 57 patients. The average number of suspicious lymph nodes per patient was 4. Among the 57 individuals included in the study, 30 (52.6%) exhibited level 1, 19 (33.3%) displayed level 2, 5 (8.7%) displayed level 3, 2 (3.5%) displayed intermammary lymph nodes, and 6 (10.5%) displayed supraclavicular suspicious lymph nodes.

A biopsy was performed in 57 patients. A total of 45 patients exhibited lymph node metastases, whereas the remaining 12 patients exhibited reactive lymph node hyperplasia.

Diagnostic Performance of the SWE

The elasticity value of the cortex was assessed in 57 ALNs during the assessments conducted on the ALNs. Similarly, the elasticity value of the hilus was examined in 37 lymph nodes where the fatty hilus was intact. In the metastatic lymph nodes, the median values of all parameters related to SWE (Emax, Emin, Emean, and ESD) were obtained for both the cortex and hilus. Nodes exhibited a much higher prevalence of hyperplasia than reactive hyperplasia, as indicated in Table 2.

Table 3 presents the diagnostic efficacy of the max, min, and Emean values for the cortex. Three indicators possess significant diagnostic efficacy in differentiating metastatic lymph nodes from reactive

Table 1. Demographic and clinical characteristics of the study group (n=57)

Variable	Number of patients n (%)
Age, years, mean±SD	48.1±10.1
Gender	
Female	56 (98.3)
Male	1 (1.7)
Menstrual status	
Pre-menopausal	29 (50.1)
Post-menopause	27 (47.4)
Not applicable (male)	1 (1.7)
Symptoms	
Breast lump	57 (100)
Mastalgia	12 (21)
Nipple retraction	5 (8.7)
Nipple discharge	2 (3.5)
Duration of symptoms, months, mean±SD	6.0±0.9
Location of the breast mass (dial)	
Upper outer	37 (64.9)
Upper interior	5 (8.7)
Lower outer	6 (10.5)
Bottom interior	5 (8.7)
Central	4 (7)
T staging	
cT2	24 (42.1)
cT3	14 (24.5)
cT4b	16 (28)
cT4c	3 (5.2)
N staging	
cN1	36 (63.1)
cN2a	8 (14)
cN3a	6 (10.5)
cN3b	2 (3.5)
cN3c	5 (8.7)
M staging	
B.C	49 (85.9)
M1	8 (14)
Histological subtype	
Invasive carcinoma	54 (94.7)
Mucinous carcinoma	3 (5.2)
Molecular subtype	
Luminal	22 (38.59)
HER2/neu	15 (26.3)
Basal	20 (35)

SD: Standard deviation

hyperplasia. Although the area under the curve (AUC) was maximum for max, the difference between Emin and Emean was not significant (p=0.73 and p=0.40, respectively). The optimal threshold values for max, min, mean, and ESD of the cortex, which can effectively differentiate metastatic from reactive hyperplasia, were 14.9, 12.2, 13.3, and 1 kPa, respectively. Owing to the obliteration of the fatty hilus in some ALNs, the diagnostic power of SWE could not be fully evaluated in all ALNs.

Table 2. Comparison of quantitative shear wave elastography parameters and B-Mode ultrasound features of lymph nodes according to pathological status (n=57)

Parameter	Nodal status at the core biopsy		p value
	Metastasis	Reactive hyperplasia	
SWE of the cortex	**n=45**	**n=12**	
Emax (kPa)	25.1 (13.8-44.7)	12.9 (11.2-15.3)	0.001
Emin (kPa)	21.45 (11.2-37.1)	10.5 (8.2-10.9)	0.002
Emean (kPa)	24.15 (13.5-42.7)	11.9 (9.2-12.8)	0.001
ESD (kPa)	1.7 (1.4-2.4)	0.95 (0.87-1.9)	0.03
SWE of the hilus	**n=27**	**n=10**	
Emax (kPa)	31.9 (18.8-44.6)	14.9 (9.5-18.1)	0.004
Emin (kPa)	29.5 (17.1-41.2)	8.5 (8.4)-14	0.004
Emean (kPa)	32.6 (19-42.9)	12.4 (8.1-15.8)	0.002
ESD (kPa)	1.9 (1.2-3.2)	0.95 (0.76-1.6)	0.008
B-Mode US features	**n=45**	**n=12**	
Cortical thickness in mm	11.55 (8.5-12.2)	7 (5.6-7.7)	<0.001
Absence of fatty hilum	40 (88.8%)	5 (41.6%)	0.004
Non-hilar blood flow	32 (71.1%)	4 (33.3%)	0.01
Round shape	14 (31.1%)	0	0.05

Each value is depicted as median (interquartile range).
SWE: Shear wave elastography, US: Ultrasonography

Table 3. Diagnostic performance of quantitative SWE and B-Mode US of axillary lymph nodes according to the pathological status of the lymph nodes (n=57)

Variables	AUC	Cut-off	TP	F.P.	TN	F.N.	Sensitivity, % (95% CI)	Specificity, % (95% CI)	LR+ (95% CI)
SWE of the cortex									
Emax	0.870	14.1 kPa	30	5	11	13	71.7 (56-87)	83.4 (53.6-92.9)	4.3 (1.45-12.1)
Emin	0.832	10.2 kPa	32	4	9	12	74.3 (63.4-85)	83.5 (51.3-92.9)	4.4 (1.6-12.6)
Emean	0.896	12.8 kPa	33	5	9	10	75.7 (63.8-89)	64.2 (54.6-95.7)	4.3 (1.4-11.2)
ESD	0.782	1 kPa	35	8	7	7	82.3 (68.3-90.9)	52.5 (29-80.6)	1.8 (1.3-2.9)
B-Mode US features									
Cortical thickness	0.968	6.4 mm	37	5	10	5	89.5 (75.9-95.8)	72.7 (43.4-90.3)	3.3 (1.7-6.3)
Absence of fatty hilum	-	-	37	4	9	7	82.1 (71.4-92.6)	65.6 (345-84.1)	2.5 (1.6-3.9)
Non-hilar blood flow	-	-	32	5	10	10	74.6 (59.4-80.7)	73.9 (44.8- 92.3)	2.4 (1.4-5.8)
Cortical thickness + effacement of fatty hilum and/or non-hilar blood flow	-	≥6.4 mm	38	3	11	5	88.1 (76.7-94.8)	92.1 (63.4-98.6)	9.6 (1.5-72.4)
Combination of SWE and B-Mode US									
Emax (cortex) + cortical thickness	-	≥14.1 kPa + ≥6.4 mm	30	2	11	14	64.9 (48.1-79.8)	92.9 (64.1-97.2)	7 (1-51.8)
Emax (cortex) + cortical thickness + effacement of fatty hilum and/or non-hilar blood flow	-	≥14.1 kPa + ≥6.4 mm	29	0	14	14	67.5 (51.9-79.6)	100 (75.2-100)	-

AUC: Area under the curve, CI: Confidence interval, FN: False negatives; FP: False positives, LR+: Positive likelihood ratio, kPa: Kilo pascal, SWE: Shear wave elastography, TN: True negatives, TP: True positives, US: Ultrasonography

Diagnostic Power of B-Mode US

Metastatic lymph nodes had a higher prevalence of prominent fatty hilus (32/45) than reactive lymph nodes (4/12) (p=0.004). The prevalence of non-hilar engorgement was higher in cases of metastasis (32 out of 45) than in cases of reactive hyperplasia (4 out of 12) (p=0.01). The round shape of lymph nodes was observed in metastatic lymph nodes (14/45) but not reactive lymph nodes (0/12). Although not observed, the difference was not statistically significant (p=0.05) (Table 2). The B-Mode US of cortical thickness demonstrated the highest sensitivity and specificity, with an AUC of 0.87. A threshold value of 6.4 mm was determined to be the most effective value for differentiating metastatic lymph nodes from reactive hyperplasia, with a sensitivity and specificity of 89.5% and specificity of 72.7%. The combined evaluation of lymph nodes with cortical thickness >6.4 mm, non-cortical blood supply, and fatty hilus resulted in a sensitivity of 89.5% and specificity of 90.9% (Table 3). A comparative analysis was conducted to assess the specificity and sensitivity of the Emax value of the cortex, which is considered the parameter with the highest diagnostic power in SWE, in relation to the B-Mode US features of the ALNs. The Emax of the cortex exhibited a higher degree of specificity than the cortical thickness (81.8% vs. 72.7%). However, its sensitivity was found to be quite low (73.7% to 89.5%). However, the differences were not statistically significant (p=0.61 and 0.08, respectively).

Diagnostic Power of the B-Mode US and SWE

The evaluation utilized a combination of cortical thickness in B-Mode US and the Emax value of the cortex in SWE because these parameters demonstrated the strongest diagnostic power. When the Emax value of the cortex was combined with 14.1> kPa, the specificity of the lymph nodes measured with a cortex thickness >6.4 mm increased (72.7-90.9%) (p=0.27), its sensitivity decreased (89.5%-65.8%) (p=0.01). Similarly, when at least two B-Mode US features (non-hilar blood flow and cortical thickness >6.7 mm) were combined with the Emax value of the cortex, specificity increased (increased from 90.0% to 100%) (p=0.31), and sensitivity decreased (from 89.5% to 65.8%) (p=0.01). The specificity was found to be equal (90.9%) between the combination of Emax of the cortex and cortical thickness, as well as between at least two B-Mode US characteristics. However, the sensitivity was significantly lower (65.8-90.5%) (p=0.01) (Table 3).

Discussion

US-guided biopsy is a widely used technique for evaluating ALNs in individuals diagnosed with breast cancer. However, our study revealed a false-positive result when assessing the cortical thickness of ALNs. Compared with the biopsy results for these lymph nodes, reactive hyperplasia was detected in 12 of 57 lymph nodes (21%). Therefore, additional studies are necessary to evaluate the level of specificity exhibited by US. Therefore, this study aimed to evaluate the diagnostic effectiveness of SWE and US.

To differentiate reactive hyperplasia from metastatic lymph nodes, we assessed lymph nodes exhibiting heightened cortical thickness using a combination of B-Mode US and SWE. Subsequently, we compared these lymph nodes with B-Mode US features to ascertain the practical advantages of SWE.

The most influential criterion for differentiating reactive hyperplasia from metastasis among the B-Mode US features of the ALN was increased cortical thickness. The examined patients exhibited a substantial number of ALNs, with a cut-off value of 6.4 mm. This cut-off value achieved sensitivity of 92% sensitivity and 73.4% specificity. Different cut-off values have been reported in various studies due to differences in patient groups and study environments. Zhu et al.[18] determined that a cortical thickness of 3.5 mm was optimal for predicting metastasis. Using this threshold, they attained a sensitivity of 76% and a specificity of 83%. Seo and Sohn[19] determined that a cortical thickness cut-off value of 4.85 mm is sufficient for predicting metastasis in patients with breast cancer. With this cut-off value, they achieved 82.4% sensitivity and 100% specificity. In the current study, a higher cut-off value was used owing to the large number of ALNs.

The cortex of metastatic lymph nodes exhibited greater hardness in comparison to benign lymph nodes in our study. It was found that the hilus and cortex exhibited higher flexibility. The investigation revealed that the Emax values of the cortex and hilus were elevated in metastatic lymph nodes compared with reactive hyperplasia. This study determined that the Emax value of the cortex exhibited the highest significance in differentiating between metastasis and reactive hyperplasia. This parameter had a sensitivity of 71.7% and a specificity of 83.4% when measured at a pressure of 14.1 kPa. Prior research has demonstrated that the Emax and Emin values of the cortex have significant predictive ability in determining metastasis.[16-20] Prior research used ROI values ranging from 2 to 3 mm to assess the level of hardness. However, in our investigation, we used ROI values below 1 mm. In previous investigations, lymph nodes exhibiting normal cortical thickness of the ALNs were also incorporated into the analysis. However, our study exclusively focused on lymph nodes with augmented cortical thickness. In the current study, the Emax value of the cortex exhibited higher specificity (83.4%) and less sensitivity (71.7%) than the lymph node cortical thickness. However, these findings were not statistically significant. Luo et al.[21] reported that the Emax value of the cortex exhibited higher specificity (88.5% versus 82%) and sensitivity (93.3% versus 91.7%) than the US. Seo and Sohn[19] it was observed that Emax values of the cortex showed comparable sensitivity (82.4% for both factors) compared with US, but decreased specificity (100% vs. 95%). Although no statistical comparison was made in these studies, SWE parameters were shown to have comparable effectiveness to B-Mode US for detecting metastatic lymph nodes. In the present investigation, it was shown that the use of SWE and US exhibited a notable degree of specificity, but was accompanied by a decline in sensitivity in the identification of metastatic lymph nodes. A high specificity of 92.9% was achieved when evaluating a cut-off value of 6.4 in conjunction with cortical thickness, while considering an Emax value of 14.1 kPa for the cortex. When evaluating ALNs using US, the specificity of lymph nodes with few suspicious findings can be increased to 100% by combining these findings with the Emax values of the cortex. Kilic et al.[16] they conducted an ex vivo study and observed that B-Mode US features, including the cortical thickness of the lymph node and long-axis/short-axis ratio, exhibited 100% specificity when evaluated together with the Emax of the cortex. However, their findings revealed a sensitivity of 34%, which is consistent with the results of our study. Kilic et al.[16] in his study, evaluating the cortical thickness and stiffness of the lymph node together resulted in a higher sensitivity of 83%, whereas a sensitivity of 75% was obtained by using each of the US parameters alone.

Additionally, our study compared the diagnostic efficiency of the combination of SWE and US and evaluated the usability of SWE using many US features. When the Emax value of the cortex was compared with the lymph node cortical thickness, it was shown that the

combination of the cortical thickness and other US parameters of the lymph node showed similar specificity and better sensitivity. Therefore, the effectiveness of SWE is limited in cases in which many suspicious features are present in the lymph nodes.

Nevertheless, previous studies have indicated that the utilization of SWE can be advantageous in cases in which cortical thickness is the sole characteristic observed in lymph nodes that are deemed worrisome. Fischer et al.[22] investigated the application of SWE in ALNs. The researchers observed that the use of cortex elasticity exhibited superior sensitivity and specificity in distinguishing between metastases and reactive hyperplasia compared with subjective evaluation using B-Mode US or elastography. The sensitivity and specificity values obtained were 95% and 74% for B-Mode US, 85% and 60% for subjective elastography, and 85% and 68% for subjective elastography.

Study Limitations

This study has several limitations. The primary constraint of our study was the limited study population size, which necessitated validation with larger study groups. The evaluation of the effectiveness of quantitative elastography was hindered by the absence of a consistent range across all the lymph nodes assessed. Further studies are required to ascertain the optimal range of elasticity that should be employed for the examination of ALNs. SWE measurements were performed by one researcher because this situation did not allow us to evaluate interobserver agreement and repeatability. Another limitation was that excisional biopsy was not performed in the 12 patients with reactive hyperplasia, as indicated by the core biopsy results, which may not represent the entire lymph node.

Conclusion

In conclusion, the use of SWE is advantageous in distinguishing between metastases and reactive hyperplasia in individuals exhibiting suspicious features on B-Mode US of ALNs. Based on our observations, the simultaneous use of SWE and B-Mode US can provide advantageous results only in cortical-thick lymph nodes.

Ethics

Ethics Committee Approval: Erzincan Binali Yıldırım University Clinical Researches Ethics Committee, 16.05.2024, EBYU KAEK 2024.05-1.2356093-113.

Informed Consent: The study was initiated after obtaining written informed consent from the patients.

Financial Disclosure: The author declared that this study received no financial support.

References

1. Bray F, Ferlay J, Soerjomataram I, Siegel RL, Torre LA, Jemal A. Global cancer statistics 2018: GLOBOCAN estimates of incidence and mortality worldwide for 36 cancers in 185 countries. CA Cancer J Clin. 2018;68:394-24.
2. Rosen RD, Sapra A. TNM Classification. on StatPearls; StatPearls Publishing LLC.: Treasure Island, FL, USA, 2022.
3. Fisher B, Bauer M, Wickerham DL, et al. Relation of number of positive axillary nodes to the prognosis of patients with primary breast cancer. An NSABP update. Cancer. 1983;52:1551-7.
4. Sutherland CM, Mather FJ. Long-term survival and prognostic factors in breast cancer patients with localized (no skin, muscle, or chest wall attachment) disease with and without positive lymph nodes. Cancer. 1986;57:622-9.
5. Rahbar H, Partridge SC, Javid SH, Lehman CD. Imaging axillary lymph nodes in patients with newly diagnosed breast cancer. Curr Probl Diagn Radiol. 2012;41:149-58.
6. Choi YJ, Ko EY, Han BK, Shin JH, Kang SS, Hahn SY. High-resolution ultrasonographic features of axillary lymph node metastasis in patients with breast cancer. Breast. 2009;18:119-22.
7. Alkuwari E, Auger M. Accuracy of fine-needle aspiration cytology of axillary lymph nodes in breast cancer patients: a study of 115 cases with cytologic-histologic correlation. Cancer. 2008;114:89-93.
8. Sianesi M, Ceci G, Ghirarduzzi A, et al. Use of axillary ultrasonography in breast cancer: a useful tool to reduce sentinel node procedures. Ann Ital Chir. 2009;80:315-8.
9. Balasubramanian I, Fleming CA, Corrigan MA, Redmond HP, Kerin MJ, Lowery AJ. Meta-analysis of the diagnostic accuracy of ultrasound-guided fine-needle aspiration and core needle biopsy in diagnosing axillary lymph node metastasis. Br J Surg. 2018;105:1244-53.
10. Houssami N, Ciatto S, Turner RM, Cody HS, Macaskill P. Preoperative ultrasound-guided needle biopsy of axillary nodes in invasive breast cancer: meta-analysis of its accuracy and utility in staging the axilla. Ann Surg. 2011;254:243-51.
11. Dietrich CF, Bamber J, Berzigotti A, et al. EFSUMB Guidelines and Recommendations on the Clinical Use of Liver Ultrasound Elastography, Update 2017 (Long Version). Ultraschall Med. 2017;38:e48.
12. Shiina T, Nightingale KR, Palmeri ML, et al. WFUMB guidelines and recommendations for clinical use of ultrasound elastography: Part 1: basic principles and terminology. Ultrasound Med Biol. 2015;41:1126-47.
13. Gao L, Parker KJ, Lerner RM, Levinson SF. Imaging of the elastic properties of tissue--a review. Ultrasound Med Biol. 1996;22:959-77.
14. Garra BS, Cespedes EI, Ophir J, et al. Elastography of breast lesions: initial clinical results. Radiology. 1997;202:79-86.
15. Ying L, Hou Y, Zheng HM, Lin X, Xie ZL, Hu YP. Real-time elastography for the differentiation of benign and malignant superficial lymph nodes: a meta-analysis. Eur J Radiol. 2012;81:2576-84.
16. Kilic F, Velidedeoglu M, Ozturk T, et al. Ex Vivo Assessment of Sentinel Lymph Nodes in Breast Cancer Using Shear Wave Elastography. J Ultrasound Med. 2016;35:271-7.
17. Chang W, Jia W, Shi J, Yuan C, Zhang Y, Chen M. Role of Elastography in Axillary Examination of Patients With Breast Cancer. J Ultrasound Med. 2018;37:699-707.
18. Zhu Y, Zhou W, Zhou JQ, et al. Axillary Staging of Early-Stage Invasive Breast Cancer by Ultrasound-Guided Fine-Needle Aspiration Cytology: Which Ultrasound Criteria for Classifying Abnormal Lymph Nodes Should Be Adopted in the Post-ACOSOG Z0011 Trial Era? J Ultrasound Med. 2016;35:885-93.
19. Seo M, Sohn YM. Differentiation of benign and metastatic axillary lymph nodes in breast cancer: additive value of shear wave elastography to B-mode ultrasound. Clin Imaging. 2018;50:258-63.
20. Tourasse C, Dénier JF, Awada A, Gratadour AC, Nessah-Bousquet K, Gay J. Elastography in the assessment of sentinel lymph nodes prior to dissection. Eur J Radiol. 2012;81:3154-9.
21. Luo S, Yao G, Hong Z, et al. Qualitative Classification of Shear Wave Elastography for Differential Diagnosis Between Benign and Metastatic Axillary Lymph Nodes in Breast Cancer. Front Oncol. 2019;9:533.
22. Fischer T, Peisker U, Fiedor S, et al. Significant differentiation of focal breast lesions: raw data-based calculation of strain ratio. Ultraschall Med. 2012;33:372-9.